



Universität  
Rostock



Traditio et Innovatio



SOLENT  
UNIVERSITY  
SOUTHAMPTON



Zachodniopomorski  
Uniwersytet  
Technologiczny  
w Szczecinie



# Development of a methodology for CFD calculations in self propulsion (propeller and waterjet)

Submitted on 31st August 2020 by Huon de Kermadec Nolwenn | 45 route de Mespaul | 29420 St Pol de Léon | [nol.dekermadec@gmail.com](mailto:nol.dekermadec@gmail.com)



*This Master Thesis has been prepared as part of the graduation of the Master in Marine Technology specialized in Hydrodynamics for Ocean Engineering from Centrale Nantes and the graduation of the double Master degree Liège University-Centrale Nantes in the EMship+ programme*

# CONTENT

---

Declaration of authorship .....	3
Abstract .....	4
Résumé.....	4
Acknowledgements.....	5
1 Objective/Contextualisation .....	6
2 FineMarine .....	7
2.1 Hexpress .....	7
2.2 Solver ISIS .....	8
2.3 CFView .....	9
3 Methodology of CFD calculations .....	10
3.1 Resistance.....	10
3.2 Self-Propulsion.....	11
4 Correlation of the results between Towing Tank and CFD .....	20
4.1 Towing Tank Test.....	20
4.2 CFD.....	21
4.3 Results .....	22
4.4 Conclusion .....	41
5 Power Prediction Methodology .....	43
5.1 Classical methodology based on resistance simulation .....	43
5.2 Adaptation with self-propulsion CFD .....	45
5.3 Results .....	45
6 Auxiliary computations .....	51
6.1 Water-Jet simulation .....	51
6.2 Resistance on Regular wave with Actuator Disk .....	53
6.3 Bollard Pull calculation .....	57
6.4 Manoeuvrability (Turning Circle).....	59
7 Discussion/Conclusion.....	61
8 References.....	62

## DECLARATION OF AUTHORSHIP

---

I declare that this thesis and the work presented in it are my own and have been generated by me as the result of my own original research.

Where I have consulted the published work of others, this is always clearly attributed.

Where I have quoted from the work of others, the source is always given. With the exception of such quotations, this thesis is entirely my own work.

I have acknowledged all main sources of help.

Where the thesis is based on work done by myself jointly with others, I have made clear exactly what was done by others and what I have contributed myself.

This thesis contains no material that has been submitted previously, in whole or in part, for the award of any other academic degree or diploma.

I cede copyright of the thesis in favour of the University of Centrale Nantes

Date: 29/08/2020

Signature

A handwritten signature in black ink, consisting of a stylized, cursive script.

## ABSTRACT

---

In the framework of the master EMship, I have performed my master thesis in the company MAURIC (Marseille), which is a naval architecture and marine engineering office.

The purpose of my master thesis was to develop a methodology for CFD calculation in self-propulsion. The validation of the results was done by correlation of the CFD results with towing tank data available on the three studied patrol boats.

This thesis allows me to handle the CFD software FineMarine, to understand the different settings and to become autonomous on it. I have mostly read about the module Actuator Disk. A numerical model of the propeller, which allows to perform CFD self-propulsion calculations, cheaper than to model the propeller itself.

From a professional and personal point of view, this internship was very rewarding. It allows me to understand the different stages of the ship conception, in particular in hydrodynamics. I had the opportunity to better define my skills and apply them. Skills that I developed last semester in Centrale Nantes during lecture of theoretical, numerical and experimental hydrodynamics.

## RESUME

---

Dans le cadre du master EMship, j'ai réalisé ma thèse de master au sein de l'entreprise MAURIC à Marseille. Mauric est un bureau d'architecte naval et d'ingénierie marine.

L'objectif de ma thèse était de développer une méthode de calculs CFD en auto-propulsion avec l'utilisation de l'actuator disk. La validation de la méthode a été réalisée par corrélation des résultats CFD avec des données bassin disponibles sur les trois patrouilleurs étudiés.

Cette thèse m'a permis de prendre en main le logiciel de calculs CFD FineMarine, de comprendre les différents réglages et de pouvoir être autonome dessus. Je me suis documentée plus particulièrement sur le module de l'actuator disk, modèle numérique de l'hélice, qui permet de simuler des calculs en auto-propulsion de manière moins coûteuse que l'hélice elle-même.

D'un point de vue professionnel et personnel, ce stage fut très enrichissant. Il m'a permis de comprendre les différentes étapes de la conception de navire, notamment d'un point de vue hydrodynamique. J'ai pu mettre en application les compétences développées le semestre dernier à l'école Centrale Nantes lors des cours d'hydrodynamique théorique, numérique et expérimentale.

## ACKNOWLEDGEMENTS

---

I would like to deeply thank the team of Mauric Marseille. I have been very well welcomed and it was a pleasure to work daily with them.

I want to thank more specifically *Antoine Durat* who was my supervisor during this period. He took time to train me on the software FineMarine. He gave me lot of good advises about CFD, and taught me a lot about ship hydrodynamic in general.

Furthermore, I would like to thank *Jean-Charles Nahon*, former CEO of Mauric, who was my professor during my first year of EMship in Liège. He gave me my first class about ship hydrodynamics which encouraged me to continue in this field and to perform my second year in Centrale Nantes. He also helped me a lot to get this internship in giving my references to the current director, *François Sebilo*.

Finally, I want to thank the master Emship, more precisely the professors, the supervisors, *Philippe Rigo* and *Lionel Gentaz*. Those two years allow me to achieve my professional and personal goals which was to be specialized in naval engineering. I have learnt a lot during those two years, especially in the field of naval hydrodynamics that I have directly applied during this internship.

# 1 OBJECTIVE/CONTEXTUALISATION

---

Ship hydrodynamic is a very important topic when dealing with ship design. It allows to predict the performance of the ship in terms of operational speed, powering prediction, energy consumption and environmental impact. CFD has been developed since few years now, and it allows to solve different hydrodynamics problem such as resistance, seakeeping, manoeuvrability... It is becoming very reliable and it is very used in industry now since it has been very well improved to decrease the computational cost.

The main function of CFD in naval engineering is to compute the ship resistance. In ship resistance computation, the ship is towed and the forces are integrated to get the total drag. Therefore, the propulsion system is not represented.

However, in reality, the propulsion system is interacting with the hull, and this interaction tends to decrease the power transmitted to the flow through the propeller. Two main effects are observed: suction effect and wake effect. In Resistance CFD, two efficiency coefficients are determined empirically to take into account this interaction.

To represent this interaction in the computation, the idea is to integrate the propulsion system, more precisely the propeller itself. It will help to take into account these interactions and so to have a more realistic flow around the ship, and at the stern.

The objective of this master thesis is to develop a methodology to perform self-propulsion CFD calculations using a simplified model of the propeller called the Actuator Disk.

In a first part, the actuator disk was studied, in order to understand how it works, and why it has been developed. Then, using the software FineMarine, some calculations were run in order to figure out the different modules/options that are available. Some comparisons were done using towing tank results that were performed few years ago on the two patrol boats studied. Once the tool was handled, some self-propulsion calculations were launched with the currently developed patrol boat. The results were also compared to the tank results since it was done during the same period. Finally, some auxiliary CFD calculations were performed using the actuator disk such that: study of the flow around the shaft bearings, Resistance on regular wave, Bollard-Pull calculations, Manoeuvrability study.

Because of the sensitivity of the different data, the name of the name of the different ships on which I have worked are hided. Instead, for the patrol boats, they will be call: Ship A, ship B and ship C. The characteristics of the ship are not given intentionally. Moreover, regarding the different CFD results (Resistance, Trim, Sinkage..) the raw values are also not given. As in this thesis the interest is to show the correlation of the results, it has not a direct impact on the comprehension.

## 2 FINEMARINE

---

FineMarine is a software developed by the company NUMECA. It is a CFD software mainly focused on naval hydrodynamics. It is structured in three main components:

- Hexpress: Automated all-hexahedral unstructured grid generation system
- Solver ISIS: Multi-fluids solver to solve Navier-Stokes equation or Euler equations depending of the model chosen (developed by Centrale Nantes)
- CFview: Post-processing software (flow visualization)

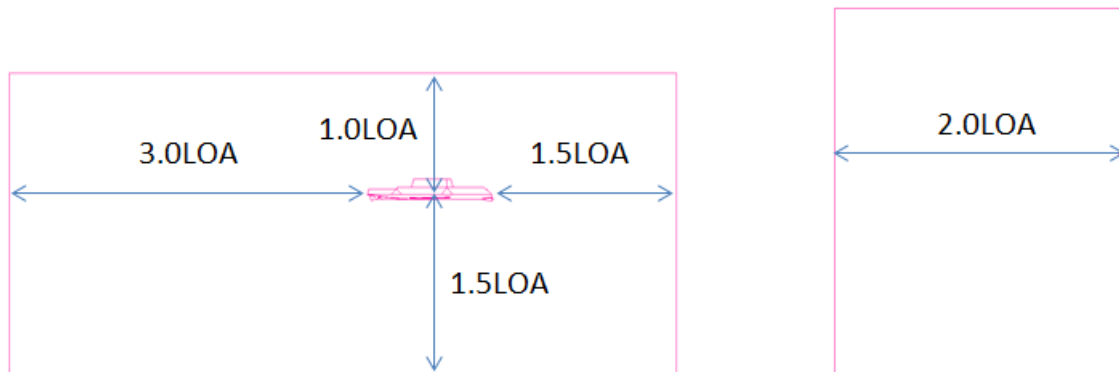
### 2.1 HEXPRESS

#### 2.1.1 Mesh step

Hexpress is an automatic unstructured mesh generator of hexahedral elements. It can be used to mesh complex 2D or 3D geometries.

After the importation of the parasolid, major steps are necessary as described below.

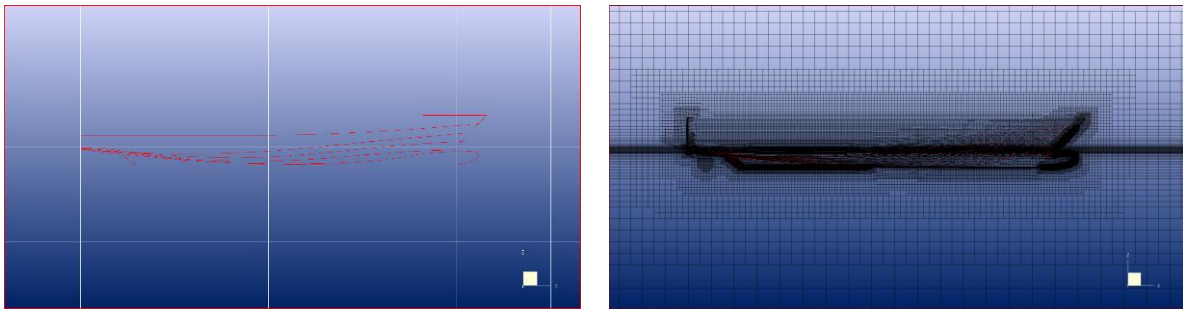
- Domain creation by triangulation of the geometry
  - The domain dimensions are defined based on the type of the ship (planning boat → quite long domain /displacement boat → domain can be shorter)



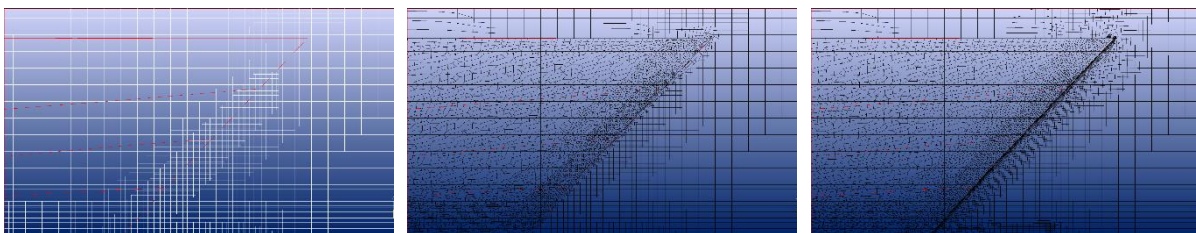
Standard Domain Size [1]

- Initial mesh
  - The initial mesh is the mesh that will be then refined around the ship hull.
  - Try to have an isotropic initial mesh in order to avoid any big deformation of the mesh.
- Mesh adaptation
  - Depending on the surfaces, a mesh refinement will be applied in order to represent as best as possible the surfaces (shape, curvature).
  - Some curves can be as well refined. It will be the fact for the short curves or at some critical location in term of the flow (leading edge, trailing edge)
  - A diffusion factor is also chosen (=4) to determine how fast the mesh size will be refined from fine to coarse cells.
- Snap Geometry:
  - Allow to project the mesh on the different surfaces to capture the geometrical features.
- Optimization

- Allow to optimize the mesh to enhance the mesh quality (avoid any bad quality elements that can stopped the solver resolution)
- Viscous layer insertion
  - If necessary, it is possible to add a viscous layer in order to capture well the viscous effects that occur near by the boundary layer.
  - $Y^+$  calculator depending on: reference velocity, reference length, fluid parameters (viscosity and density). It allows to compute the thickness of the first layer and the number of layers.



*Initial mesh (Left) to viscous layer insertion (Right)*



*Zoom on the bow: Adapt to geometry (Left), Optimization (Middle), Viscous Layer (Right)*

### 2.1.2 Mesh quality

The mesh quality is very important since it has a direct impact on the interpolation given the final results. A bad quality mesh can lead to a wrong estimation of the final values or to a failure of the solver.

The main elements to be avoided are:

- Negative cells: Cells with a negative volume. The solver cannot start if at least one cell is negative.
- Concave cells\Twisted cells: These cells are less likely to present stability or robustness issues. However, they can lead to negative cells during the solvation.

The orthogonality of the cells is also checked to be sure that the cells are not too deformed. A minimal orthogonality over  $10^\circ$  is required to ensure a good quality.

## 2.2 SOLVER ISIS

ISIS-CFD flow solver, developed by Ecole Centrale Nantes, is a solver using the incompressible unsteady Reynolds-averaged Navier Stokes equations (RANSE). The spatial discretization of the transport equations is built using a finite volume method. The RANSE equations are composed of two main set of equations: the momentum conservations equations and the continuity equations. The momentum conservations equations is used to derive the velocity field, whereas the continuity equation gives the pressure field. To



simulate turbulent flows, additional equations are added, known as closure equations. For this thesis, the turbulent model  $k - \omega SST$  is used by default. According to numeca, it represents the recommended model for all basic hydrodynamic computations.

## 2.3 CFVIEW

CFView is a software that is used to perform the post-processing part. It allows to represent the different characteristics of the flow at the end of the simulation. In general, the following characteristics are checked:

- Mass fraction on the hull
- Representation of the free surface/wave elevation
- Hydrodynamic pressure
- Magnitude of the velocity
- Streamlines near the appendices in order to validate their position/orientation

## 3 METHODOLOGY OF CFD CALCULATIONS

### 3.1 RESISTANCE

Resistance CFD simulation is a classical calculation, with many documentations. Few years ago, it was quite costly to perform CFD calculation in term of time and equipment. It has been studied for a long time, and for few year, it is applicable directly in industry since it has been improved and it takes reasonable time to run. CFD is becoming more and more reliable, and the industries are going less toward towing tank test since it takes time (preparation of the model, test) and it is much more costly.

- Why performing Resistance CFD simulation?

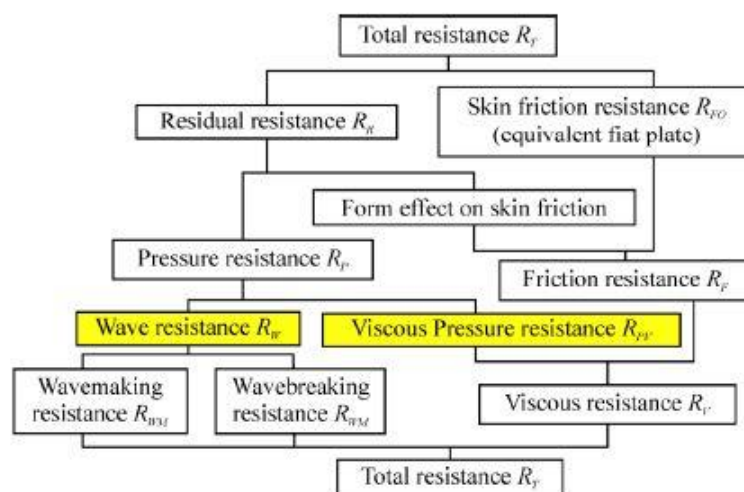
Resistance simulations are done from the very beginning of a project (tender's stage) in order to optimize the hull form such that it induces a resistance as low as possible. CFD is very useful in this stage since it allows to give good results quite quickly.

It is also performed to the final hull form with the different appendages to assess the performance prediction. Sometimes, in parallel, towing tank tests are also performed at this stage. It allows to validate the results obtained in CFD.

A low resistance is always desired since a higher resistance will lead to a higher propulsion needs, to a bigger weight due to a larger engine and to a bigger environment impact which is an important topic nowadays.

CFD resistance settings are quite simple. The simulation consists in imposing a velocity to the ship (imposed Tx motion), and the solver is evaluating the different forces acting on the hull to compute the total resistance. The ship is free to sink and trim. It allows the ship to reach its dynamic position (starting point=static position). The propulsion effort is located at the gearbox location.

The ship resistance is mainly influenced by the speed, the displacement and the hull form. The total resistance consists of many source-resistance as shown in the graph below.



Source-resistances [2]

According to Froude theory developed on ship resistance, the two main source-resistances are: Residual resistance and Frictional resistance. The definitions are given below. [3]

- Residual resistance: It is caused by the distribution of pressure which develops along the hull due to the waves and eddies created by the ship's motion.
- Frictional resistance: It is caused by tangential stresses due to the drag of the water moving parallel to the hull's surface.

## 3.2 SELF-PROPULSION

### 3.2.1 Introduction

Nowadays, more and more research are done on self-propulsion CFD simulation. Self-Propulsion simulations consist in doing resistance calculation but in introducing the propulsion system. It allows to simulate the interaction between the hull and the propeller that is hidden in simple resistance test.

The standard way to do it would be to implement the real propeller and to impose its rotation. This solution requires significant computational resource since a small time step is required in order to resolve the unsteady interaction between the hull and the propeller by the sliding mesh method, and it requires a more complex mesh [4].

Therefore, an alternative way is used here. Instead of modelling the real propeller, a numerical model of it is implemented called the Actuator disk.

### 3.2.2 Actuator disk

The Actuator disk is like an infinite blade model where the time averaged fluid dynamic action of the propeller are represented through body forces in the RANSE solver [5]. Theoretically, the thrust is evaluated from the pressure jump through the disk and the torque from the velocity swirl jump [6]. As it is represented by an infinite blade propeller, the nonuniformity due to the presence of the blades and tip losses are not directly taken into account.

An Actuator disk model is already implemented in FineMarine software and will be directly used in the following sections. Several configurations are set and the main equations will be given later on. The configuration chosen depends mainly on the input/output desired. The geometry of the disk is based on the real propeller geometrical characteristics such that: inner/outer radius, thickness, centre coordinates, direction. In order to well-captured the flow in the disk volume, a refinement has to be applied at its location. It will allow to have a mesh as uniform as possible. According to Numeca, at least 20 cells should be present in the thickness of the disk [1].

### 3.2.3 Mathematical model

As mentioned earlier, the actuator disk is a physical model of the real propeller of a ship. Some forces are added in the area of the disk that are representing by source terms added in the RANSE equations. These source terms are directly linked to the thrust and torque generated by the disk. The default source terms are described below.

The axial force is given by the following formula:

$$f_{bx} = A_x r^* \sqrt{1 - r^*}$$

The tangential force is given by this second formula:

$$f_{b\theta} = A_\theta \frac{r^* \sqrt{(1 - r^*)}}{r^* (1 - r'_h) + r'_h}$$

This term is taken into account only when the user activates the tangential force in the solver. It allows to add the swirl effect of the propeller on the flow caused by the rotation of the propeller.

Where the parameters are defined such as:

- $r^* = \frac{r' - r'_h}{1 - r'_h}$  : Dimensionless radius (going from 0 to 1)
- $r'_h = \frac{R_H}{R_P}$
- $r' = \frac{r}{R_P}$
- $r = \sqrt{(y - Y_{PC})^2 + (z - Z_{PC})^2}$  : Definition of the radius
- $A_x = \frac{C_T}{\Delta} \frac{105}{16(4+3r'_h)(1-r'_h)}$  : Axial force coefficient
- $A_\theta = \frac{K_Q}{\Delta J^2} \frac{105}{\pi(4+3r'_h)(1-r'_h)}$  : Tangential force coefficient
- $J = \frac{2\pi U}{\Omega D_p} = \frac{U}{n D_p}$  : Advance coefficient
- $C_T = \frac{2T}{\rho U^2 \pi R_p^2}$  : Thrust coefficient
- $K_T = \frac{T}{\rho n^2 D_p^4}$  : Thrust coefficient (Alternative formula)
- $K_Q = \frac{Q}{\rho n^2 D_p^5}$  : Torque coefficient

The main idea of these terms is that the integration of these terms on the disk volume gives the total thrust T and total torque Q.

$$T = \rho L^2 U^2 \iint_A \int f_{bx} \, dA$$

$$Q = \rho L^3 U^2 \iint_A \int r f_{b\theta} \, dA$$

Where:

- $dA = 2\pi r \Delta dr$

The demonstrations of the formulas for  $A_x$  and  $A_\theta$  are given in a thesis given in references [7].

### 3.2.4 Type of load distribution

Several types of load distribution can be used depending on the configuration and the type of the propulsion system (classical propeller or waterjet). These distributions are explained below.

- **Default:** The source terms are varying along the radius but are independent of the angle. The distribution is given by the previous formula. The axial velocity tends to zero where the hub of the propeller should be (in the inner radius). Then, it is increasing along the blades of the propeller. The peak is occurring at 70% of the radius, and then the pressure jump is decreasing until the tip of the blade where it falls to zero. The distribution will be show in a following section and will be compared to the numerical results.
- **Constant:** The distribution of the source terms is constant over the disk area. It is mostly used when the incoming flow is concentrated by a specific device such as a ducted propeller. Furthermore, it will be used also for water-jet CFD simulation since the incoming flow is concentrated in the specific duct and so the fluid distribution will be constant over the disk area.
- **User-defined:** The user has also the possibility to define himself the distribution.

As mentioned earlier, different settings are available according to the input/output desired. The different configurations are defined below.

### 3.2.5 Body Self-Update

The option “Body self-update” is a configuration that allows to evaluate given parameters of the disk at a regular time step as function of:

- Resistance (Body Drag)
- Advance velocity and open-water propeller characteristics (Open-Water)

Both options are defined below.

#### ➤ Body Drag

In a stationary state, as stated by the first law of Newton, at the equilibrium, the longitudinal forces that are applied on the ship are compensated. Therefore, the ship drag is equal to the thrust generated by the propulsion system. Hence, the option “Body Self-Update/Body Drag” allows to evaluate, at a given frequency, the thrust force by equalizing with the resistance  $R_x$ .

With this configuration, the input data are the following:

- Thrust initial value
- Torque initial value (only if the tangential forces are set active)
- Geometrical data of the disk
- Update frequency (mostly set as one time step)

The surge motion has to be imposed in order to reach the target velocity.

If the tangential forces are not active, the thrust initial value has no influence since it will be automatically updated by the resistance value.

However, in the case of the tangential forces are active, then the initial values are very important. Indeed, the thrust will remain updated by the resistance value but the torque will be computed based on the initial ratio torque/thrust with the following rule:

$$Q = \frac{Q_0}{T_0} T$$

Hence the choice of the initial values are quite strategical. A wrong estimation of the initial values will lead to a wrong estimation of the final torque and so it will not be able to characterize correctly the swirl of the flow.

This initial value can be either known by the user or defined based on the open-water curves of the propeller.

#### ➤ Open-Water

In this configuration, the thrust and torque coefficients are directly extracted from the open-water curves. Knowing these coefficients, the solver can directly evaluate the source terms added in the control volume and to solve the Navier-Stokes equations.

In this configuration, the input data are the following:

- Open-Water curves. If these curves are not known, a software is available to generate it based on characteristics data of the propeller (Wageningen B-series).
- Rotation speed of the disk. It can be either imposed by the user or solved by the solver. The rotation direction can be chosen as clockwise and counter-clockwise.
- Geometrical data of the disk
- Update frequency (mostly set as one time step)

Two type of simulations are possible:

- The ship advance velocity is imposed and the disk rotation speed is solved.
- The disk rotation speed is imposed and the ship velocity is solved.

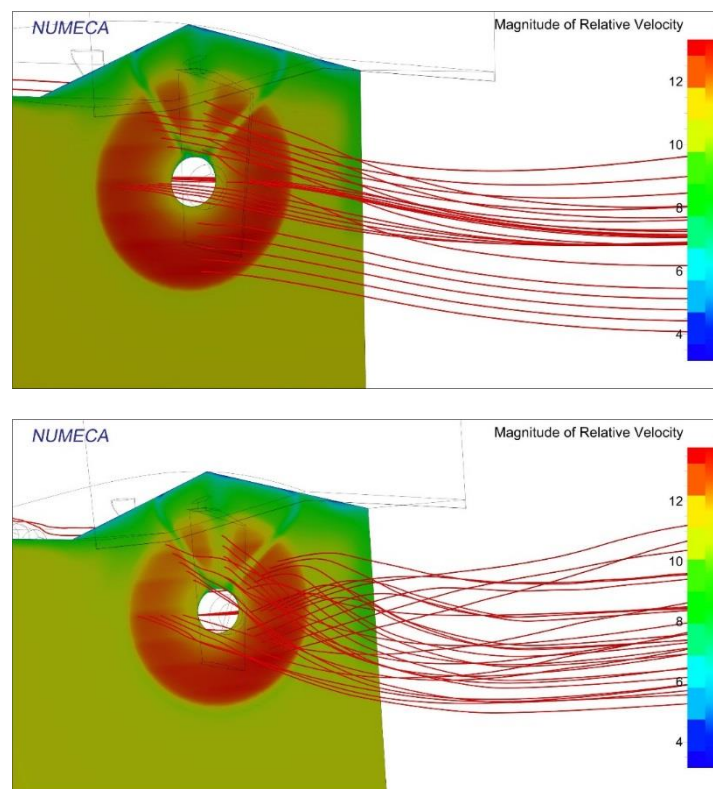
The second simulation required to know the rotation speed to reach the target speed.

### 3.2.6 Without the option "Body Self-Update"

It is also possible to use the module of the actuator disk without the "body self-update" option. In this case, the user has to define the desired thrust and torque values. The surge motion will be then released and the velocity will be computed based on the thrust value.

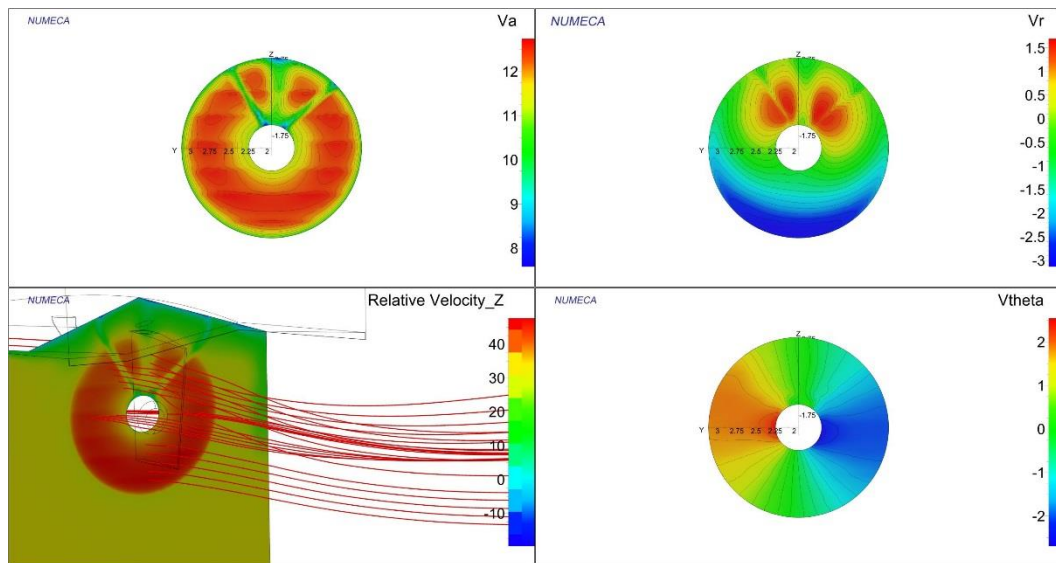
### 3.2.7 Activation of the tangential forces

As mentioned earlier, the activation of the tangential forces allows to integrate the swirl effect of the propeller to the flow due to the rotation of the propeller in the computation. Without activating those forces, only the axial forces are taken into account. In term of resistance, both configuration are providing similar results (results will be given later on). However, the activation of the tangential forces allows to get access to additional characteristics such that torque, propeller rotation speed, and to have a more realistic flow. Some comparisons of the obtained flow were done in order to assess the role of these forces on the flow itself. The images below are showing the differences. On the top, it is the flow obtained without tangential forces. As we can see, the flow is just accelerating by the disk (thrust production). On the bottom, the tangential forces are activated. And so, we can see that the propeller rotation is well simulated, and so the swirl effect is added to the flow when passing through the disk.

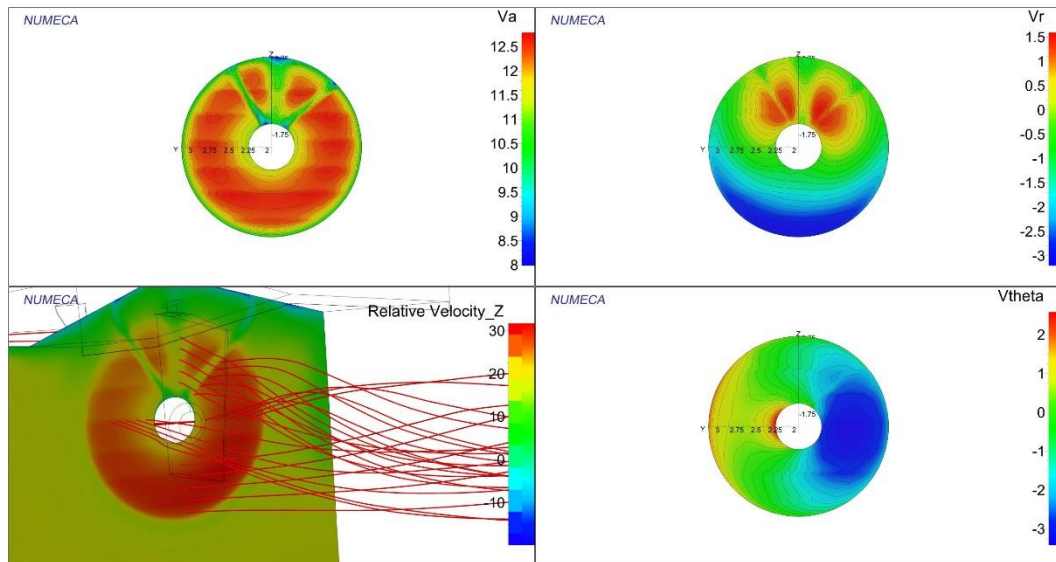


*Flow through the Actuator Disk*

The tangential force is a force that acts as the torque of the propeller. It will mainly influence on the tangential velocity field, it is why the flow is starting to swirl. Below the different velocities on the disk are shown (Axial, Radial, and Tangential).



*Wake flow without tangential force*

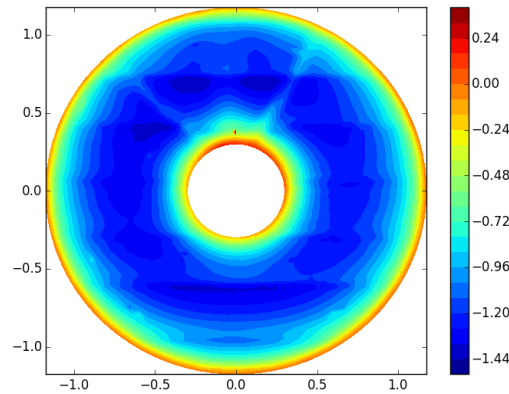


*Wake flow with tangential force*

As we can see the Axial and Radial velocities are similar, that was expected since only tangential forces are added. It has an impact only on the tangential velocity  $V_{\theta}$ . It is clear that the velocity has been modified. Without the activation of the tangential force, the velocity field is not influenced by the presence of the disk (same field observed without actuator disk). Moreover, it can be seen that the tangential velocity field is antisymmetric, therefore the resultant is null, it is why the flow is not rotating. When adding the tangential forces, the field is changed and is not anymore antisymmetric. The tangential velocity field induced by the activation of the tangential forces is shown below.

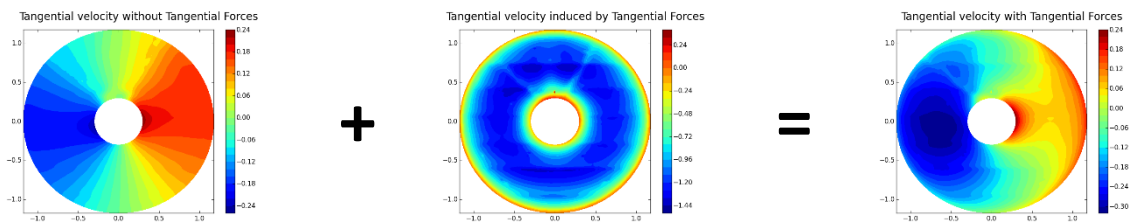


Tangential velocity induced by Tangential Forces

*Tangential velocity field induced by the activation of the tangential forces*

This figure is obtained by subtracting the velocity field with tangential forces to the one without tangential forces and it is plotted using Python. The velocity field is independent of the angle, so it means that the tangential force is applied homogeneously on the disk surface. It is adding a constant tangential velocity fields to the current one in order to make the fluid rotate. It is shown negative on the graph. In FineMarine, the positive sense is clockwise, yet here the disk is set to rotate counter clockwise, it is why a negative field is obtained.

Then this velocity field is added to the one without tangential forces to recover the field when the tangential forces are activated.

*Decomposition of the effects of the tangential forces*

### 3.2.8 Validation of the numerical results

A validation of the numerical results can be done comparing the CFD results with the theoretical equations given earlier. As mentioned earlier, through the module "Wake flow", a file can be exported containing the information about the velocity field on the disk (Axial velocity, tangential velocity, radial velocity).

- Comparison of the Axial Forces

As mentioned earlier, the axial body force is modelled by the pressure jump at the disk location ( [6], [7]). Theoretically, in FineMarine, it is computed based on the following formula:

$$f_{bx} = A_x r^* \sqrt{1 - r^{*2}}$$

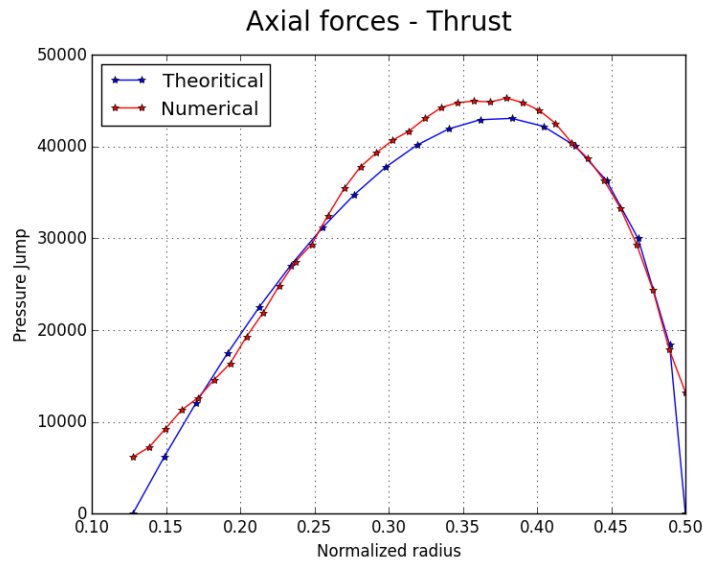
$$\leftrightarrow f_{bx} = \frac{105}{8} \frac{T}{\Delta \rho U^2 \pi R_p} \frac{1}{(4R_p + 3R_H)(R_p - R_H)} r^* \sqrt{1 - r^{*2}}$$

By dimensional analysis, we have:

$$f_{bx} = \frac{1}{\rho U^2 R_p \Delta} \Delta p$$

Numerically, in the output of Wake flow tool, we have only access to the velocity field. The pressure jump can be obtained using Bernoulli equation. Then the pressure jump is obtained by doing the difference between the field with actuator disk and without actuator disk.

The graph below shows the correlation between the theoretical results and the numerical one. It is given only for one angle ( $0^\circ$ ), and for one ship velocity (21 knots).



We can observe that there is a good correlation of the results. At both extremities, there is a major discrepancy. Normally, the forces should be equal to 0 in the CFD results as it is shown in the theoretical one. It can be due to some interpolation problem when using the wake flow tool. In fact, if the disk is in contact with the hull, then the interpolation can be wrong.

Moreover, it is possible to check that the distribution is looking like the description given earlier. The force starts to zero near the hub. Then it is increasing until 70% of the radius (maximal peak), then it starts to decrease until the tip of the blades (extremity of the disk) where the forces is null.

- Comparison of the Tangential forces

As mentioned previously, the tangential forces are computing based on the swirl velocity jump ( [6], [7]).

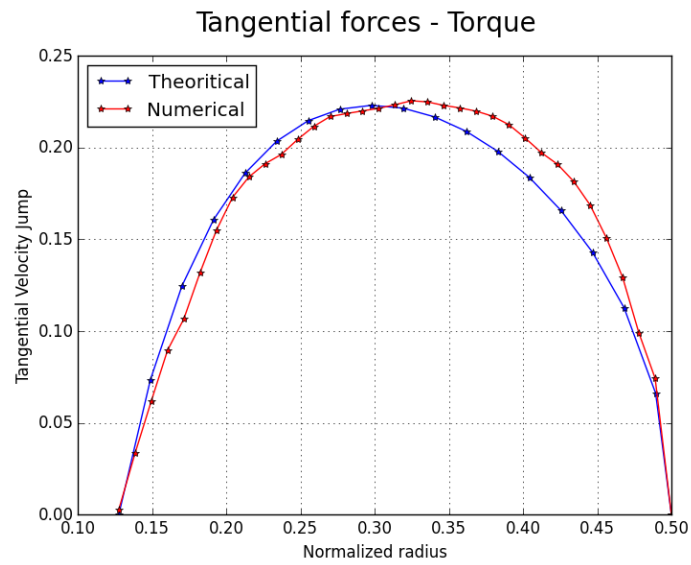
Theoretically, in FineMarine, the tangential body forces are computed based on the following formula:

$$f_{b\theta} = A_\theta \frac{r^* \sqrt{(1-r^*)}}{r^*(1-r'_h) + r'_h}$$

$$\Leftrightarrow f_{b\theta} = \frac{105 Q}{2\rho n^2 D_P \Delta J^2 \pi (4R_P + 3R_H)(R_P - R_H)} \frac{1}{r^*(1-r'_h) + r'_h} \frac{r^* \sqrt{(1-r^*)}}{r^*(1-r'_h) + r'_h}$$

Numerically, the tangential velocity is directly an output of the wake flow tool. Then the velocity jump is getting by subtracting the velocity field with actuator disk to the one without actuator disk.

Below, the graph shows the correlation between the theoretical results and the numerical one. It is given only for one angle ( $0^\circ$ ), and for one ship velocity (21 knots).



We can observe a good correlation between the theoretical and numerical results. Therefore, it validates the use of the numerical model.

## 4 CORRELATION OF THE RESULTS BETWEEN TOWING TANK AND CFD

---

### 4.1 TOWING TANK TEST

As mentioned earlier, towing tank test is a traditional way to perform resistance computation. It is done by using a scale model using Froude similitude.

The tests were performed for the three patrol boats (full appended) that are studied in this section (SHIP A, SHIP B, and SHIP C) and all the results were available in a report. Below the model used for SHIP A is shown.



*SHIP A model used for towing tank test*

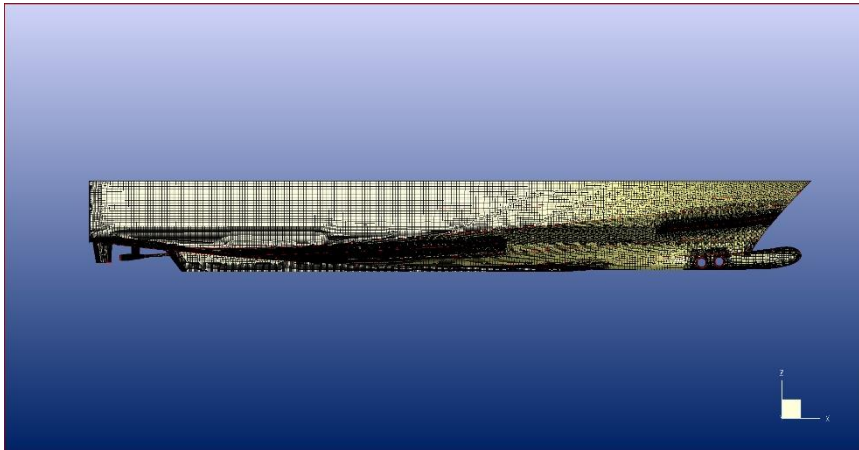
## 4.2 CFD

CFD calculations were performed as described in the previous section. They were performed under full scale, fully appended (Bow thruster, Spray rail, Bilge keel, Rudder, Shaft line, Bearings).

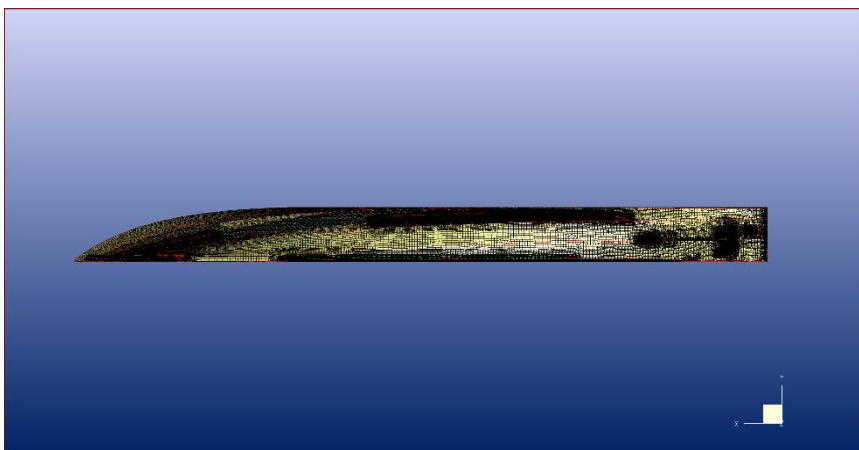
The mesh properties are given below:

	SHIP B	SHIP C	SHIP A
<b>No of cells</b>	$6,2 \cdot 10^6$	$6,3 \cdot 10^6$	$6,6 \cdot 10^6$
<b>No of concave, twisted cells</b>	0	0	0
<b>Minimum orthogonality</b>	10,7	9,5	9,3

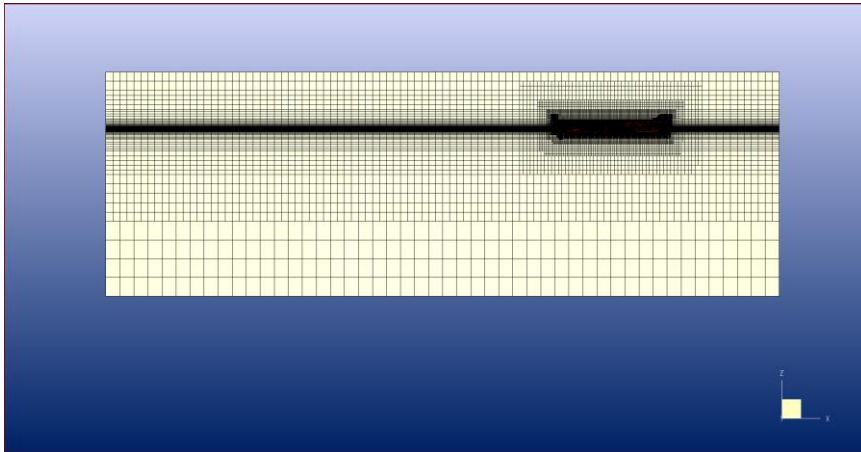
Below, some mesh views of SHIP B are shown.



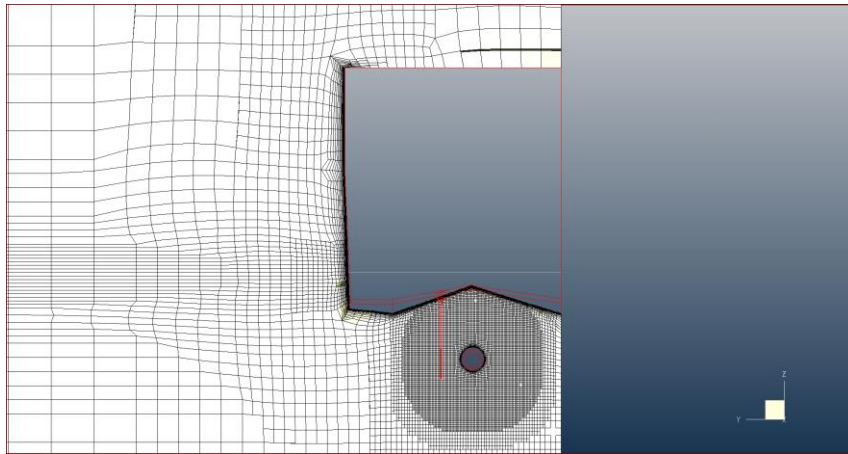
*Longitudinal view - refinement around the different appendages and free surface*



*Bottom view – refinement around the different appendages and near the actuator disk*



*Domain view – Anisotropic refinement around the free surface*



*Refinement at the actuator disk location*

### 4.3 RESULTS

In this section, the results obtained during the towing tank test and the CFD simulation are compared in order to have an order of magnitude of the gap between these two methods. This job is done for the three patrols boats. The relative errors that are computed are always based on the towing tank results.

The resistance values are always given positively. The sinkage is always negative. The trim can be negative or positive depending on the configuration and the velocity.

For self-resistance simulation, different options were used:

- Mainly body drag for SHIP B and SHIP C
- Fully Open-Water for SHIP A

#### 4.3.1 Comparaison data Towing Tank/CFD

In order to compare the CFD results with the Towing Tank results, the data must be defined by a similar way, and so the main characteristics have to be computed at the same location. Here, it is not the case of the sinkage. In fact, it is defined by two different ways:

- In FineMarine, the sinkage ( $T_z$ ) is defined as the variation of the position of the centre of gravity. The output is therefore the final position of the centre of gravity. The sinkage is then obtained by subtracting the initial position of the centre of gravity.
- In the towing tank report, the sinkage is computed as an average value of the draft computed at the bow and at the stern. It is therefore given at the midship section. In order to be able to compare the sinkage results, the idea is to re-calculate this value at the centre of gravity taking into account the trim. The following formula is applied:

$$T_{zG} = T_z + \left( LCG - \frac{LWL}{2} \right) \tan(trim[rad])$$

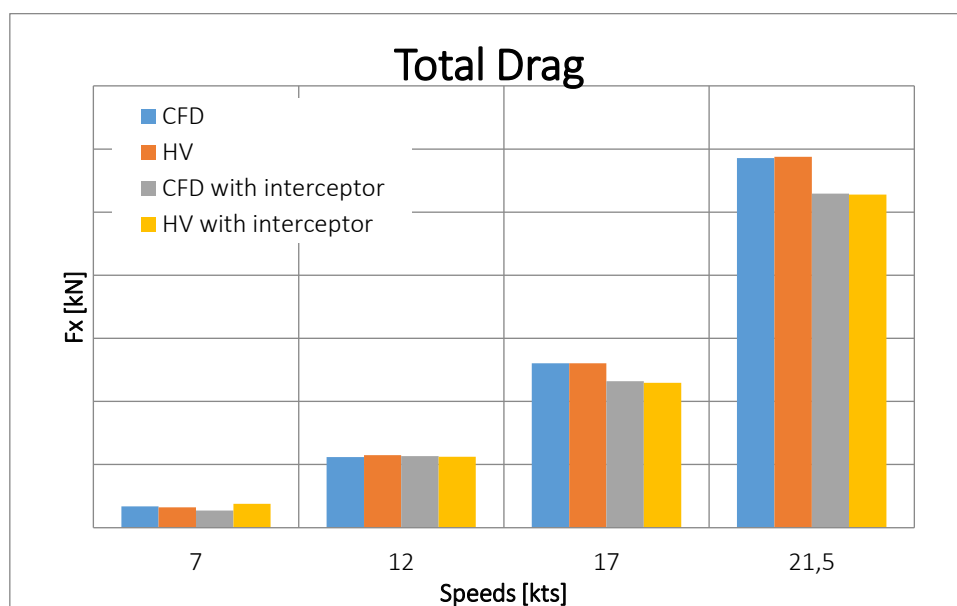
#### 4.3.2 Validation of Propulsion Settings

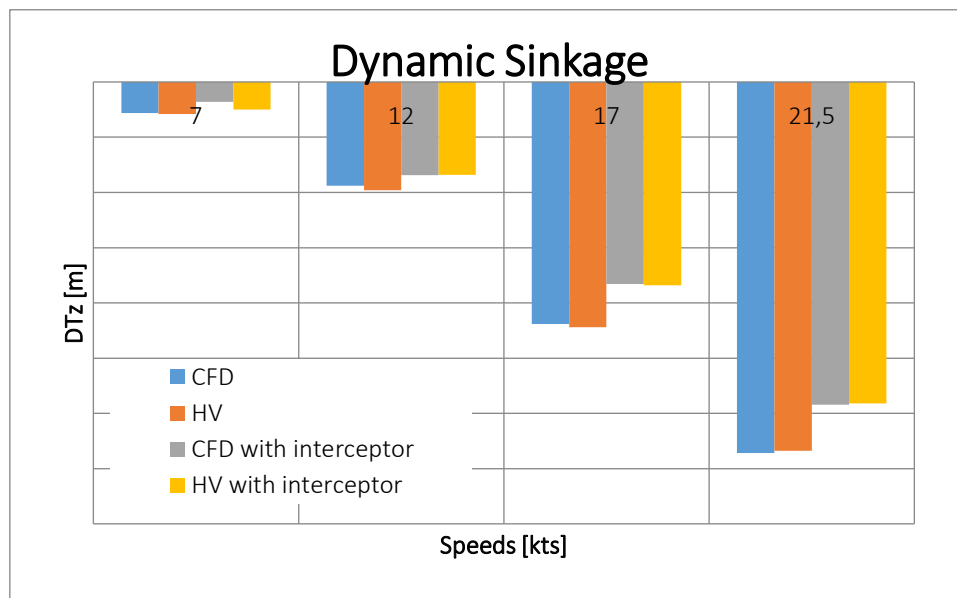
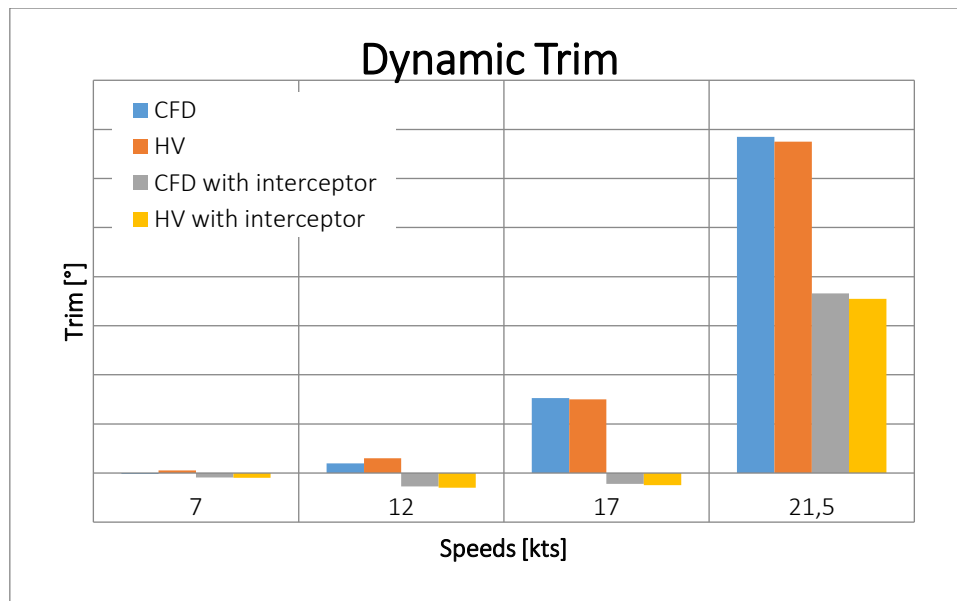
Few years ago, a study was asked to a company to perform CFD calculation on SHIP B with an actuator disk for a specific reason. Therefore, since those results were available, one idea was to compare our results with their results in order to have a first validation of the settings of the propulsion and the use of the actuator disk module. No information are provided regarding the settings of the actuator disk. Hence it will help to validate the parameters that were chosen in our case.

In the HV report, two configurations were tested:

- Without interceptor
- With an interceptor of 60mm

CFD calculations were launched in the two configurations in order to compare the results. The results are presented below. The results of the supplier are noted as HV. Our CFD results are noted CFD.





Without Interceptor

Speeds	Fx	DTz	Ry
[kts]	Relative error CFD/HV [%]	Absolute error CFD/HV [m]	Absolute error CFD/HV [°]
7	-4,49%	-0,001	0,01
12	3,30%	-0,004	0,02
17	-0,47%	-0,003	-0,01
21,5	-0,22%	0,002	-0,02



With interceptor

Speeds	Fx	DTz	Ry
[kts]	Relative error CFD/HV [%]	Absolute error CFD/HV [m]	Absolute error CFD/HV [°]
7	27,41%	-0,007	0,00
12	-1,17%	0,000	-0,01
17	-1,43%	-0,001	-0,01
21,5	-0,80%	0,001	-0,02

We can observe that in both configuration the results are very similar. For intermediate to large speeds (17-22 knots), the errors are very small (less than 1.5%). Moreover, the dynamic behaviours are similar in both cases. The absolute error in dynamic trim is less than 0,02° and in dynamic sinkage is less than 7mm. So it allows to do a first validation of the propulsion model used and of the different parameters implemented in the actuator disk module.

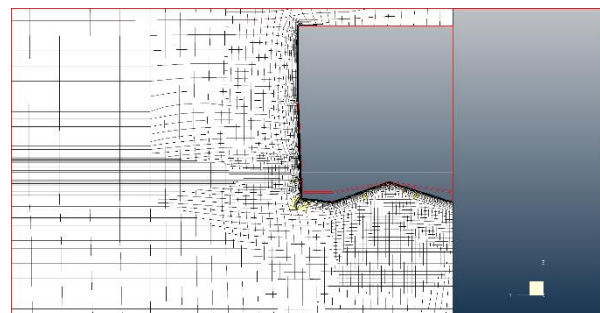
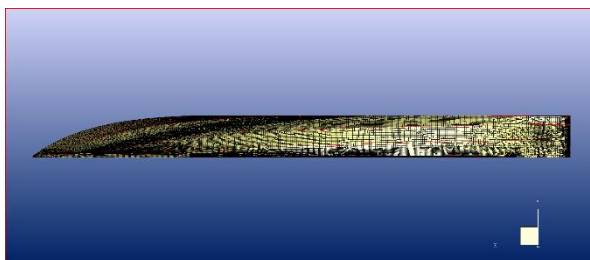
Therefore for the following, the same settings will be kept for SHIP B and the same methodology will be apply for SHIP C and SHIP A to set the actuator disk.

#### 4.3.3 Study of mesh refinement for the actuator disk

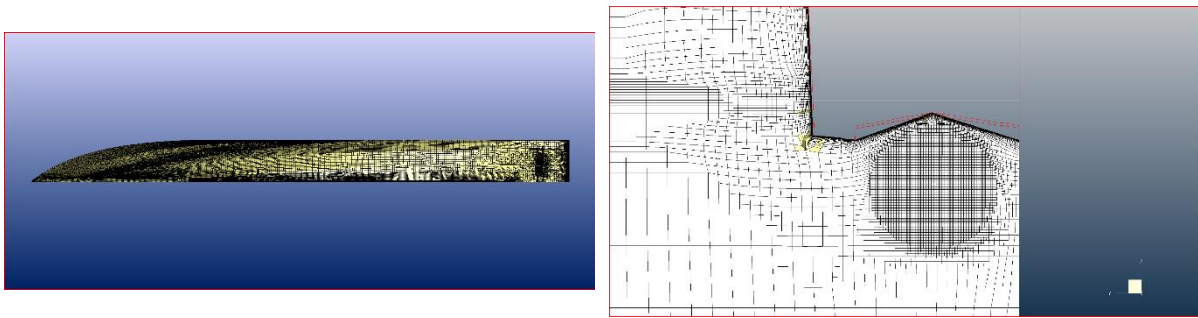
As mentioned in the introduction of the actuator disk, a sector has to be defined near the disk in order to refined the mesh, to have a mesh as uniform as possible in the disk volume. However, as we know, the number of cells has a direct impact on the cost of the calculation. Therefore, one idea here was to study the effect of the refinement on the results. For this, two meshes were done with two different refinements (7 (coarse) and 9 (fine)). To have an idea of the coefficient, the hull surfaces are refined with a coefficient of 6, and for the smallest surfaces, the refinement can be until 10. The refinement consists in a successive subdivision of the initial cells. The results are then compared to the one provided in HV report.

In FineMarine user guide [1], a refinement is advised such that there are at least 20 cells on the thickness of the disk. It would correspond to a refinement of 9 in this situation

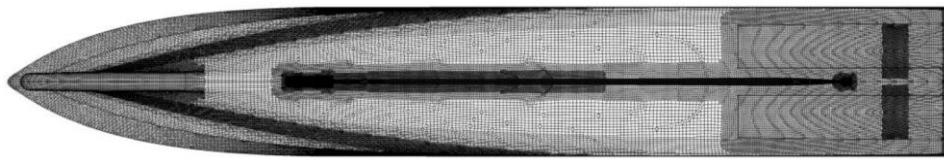
Below are shown the three different meshes that are described above.



*Coarse mesh*



Fine mesh



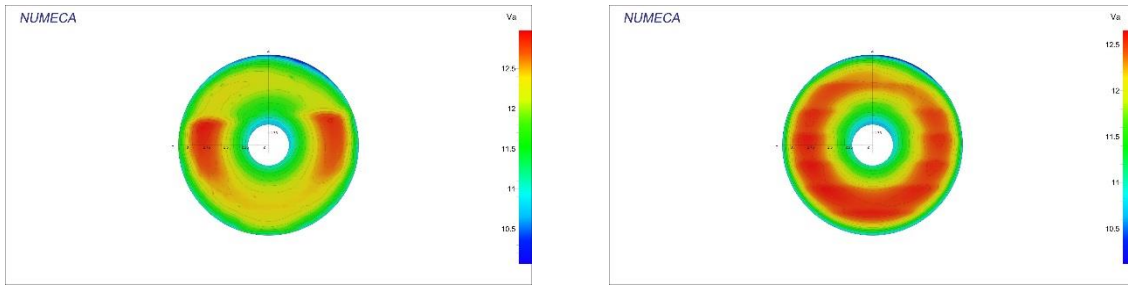
HV mesh

	Coarse Mesh	Fine Mesh
<b>No Cells</b>	2 300 000	2 700 000

Speeds [kts]	Relative error CFD/HV [%]		CPU time [h]	
	Coarse	Fine	Coarse	Fine
<b>7</b>	27,6%	27,4%	2,19	2,57
<b>12</b>	0,0%	-1,2%	3,08	3,33
<b>17</b>	-1,4%	-1,4%	6,66	8,66
<b>21.5</b>	-0,7%	-0,8%	6,47	9,08

The results obtained in both configurations are very close in term of resistance values. However, in terms of cost, it is clear that the fine mesh takes much more time to converge than the coarse mesh. It is directly linked to the increase of the number of cells.

However, not only the resistance results have to be checked. The flow has also a great important. It is required to check if a coarse mesh is enough to represent the flow through the disk. To do so the wake flow tool is used to compare the axial velocity obtained on the disk in both configurations.



Axial velocity on the disk: Coarse Mesh (left) and Fine Mesh (right)

With coarse mesh, we can observe that the flow is not uniform on the disk, the axial velocity is not well represented. It shows good results for the lateral part of the disk but not for the lower and upper part. It gives smaller velocities than with the fine mesh.

Therefore, a finer mesh allows to provide a better flow through the disk even if it adds some computational times. It is why later on, a fine refinement will be always apply for self-propulsion simulation.

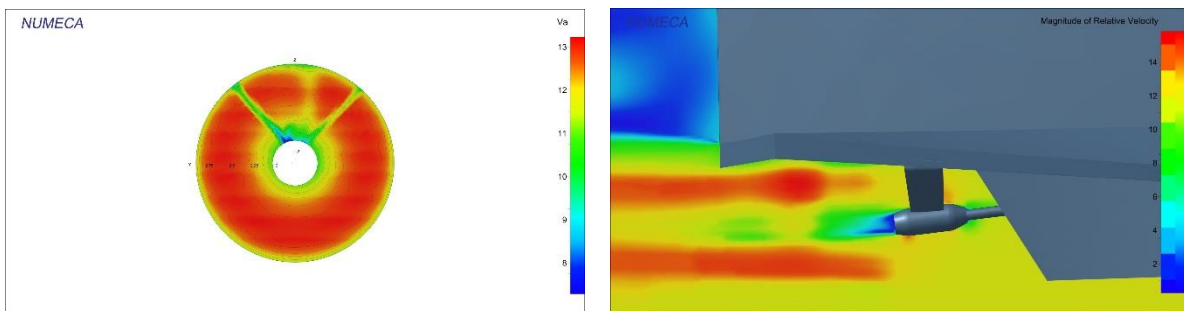
#### 4.3.4 Study of the influence of the disk thickness

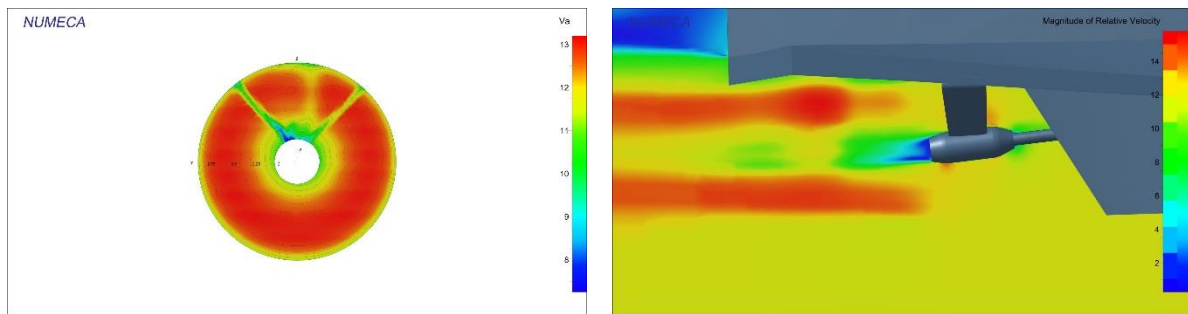
Looking at the large gap in term of thrust during the simulations that were performed, a study on the influence of the thickness of the disk was performed. Initially the thickness of the disk is taken as the thickness of the real propeller. It was thought that it may have an influence on the results, and so it was tested directly in CFD for the target speed 22 knots. Three thicknesses were tested: 0.22m, 0.3m, 0.48m.

The results are given in the table below.

Thickness	Absolute error CFD/T=0.48m	Absolute error DTz CFD/T=0.48m	Absolute error Ry CFD/T=0.48m
[m]	[kN]	[m]	[°]
<b>0,22</b>	0,13	0,001	0
<b>0,3</b>	0	0,002	0

We can clearly see that the results are very similar from one thickness to another. Hence, the thickness has not direct influence on the thrust results.





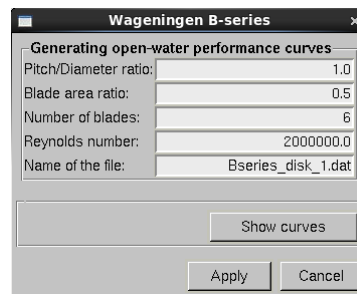
Flow visualization: Thickness of 0.3m (Top) and thickness of 0.45m (Down)

In terms of the flow, it can be seen that both thicknesses give similar results. The wake flows are similar. Therefore, the thickness just gives the control volume where the source terms will be added in the solver.

#### 4.3.5 Correlation Open-Water curves

In order to launch the self-propulsion computations with the option Open-Water the open-water curves have to be generated. Open-water curves are curves representing the evolution of the thrust coefficient  $K_T$ , the torque coefficient  $K_Q$  and the open-water efficiency  $\eta_0$  with respect to the advanced coefficient  $J$ . As mentioned earlier, if there are not known, there are two different ways to get the open-water curves:

- From a database of propeller provided by Bseries if there are not known (small software in FineMarine). The user interface is shown below:



Bseries open-water curves generator [1]

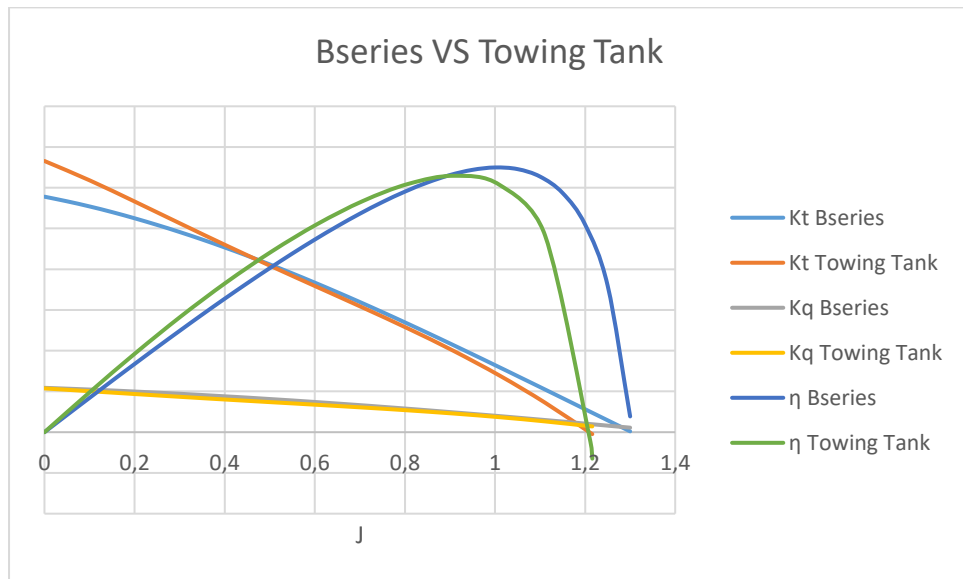
- Open-Water curves used during Towing Tank test (Provided in the supplier report). However, these curves are mostly given at model scale. ITTC provides a simple procedure to extrapolate the curves at full scale.

For SHIP B and SHIP C, the curves were generated numerically by the software in FineMarine. Therefore, it is possible to compare the curves used during CFD calculations and during the Tank test.

For SHIP A, since it is currently developed project, all the data of the propeller were not available. Then the curves from the towing tank test were used instead of using the software of FineMarine.

#### ➤ SHIP B

The results are given below.

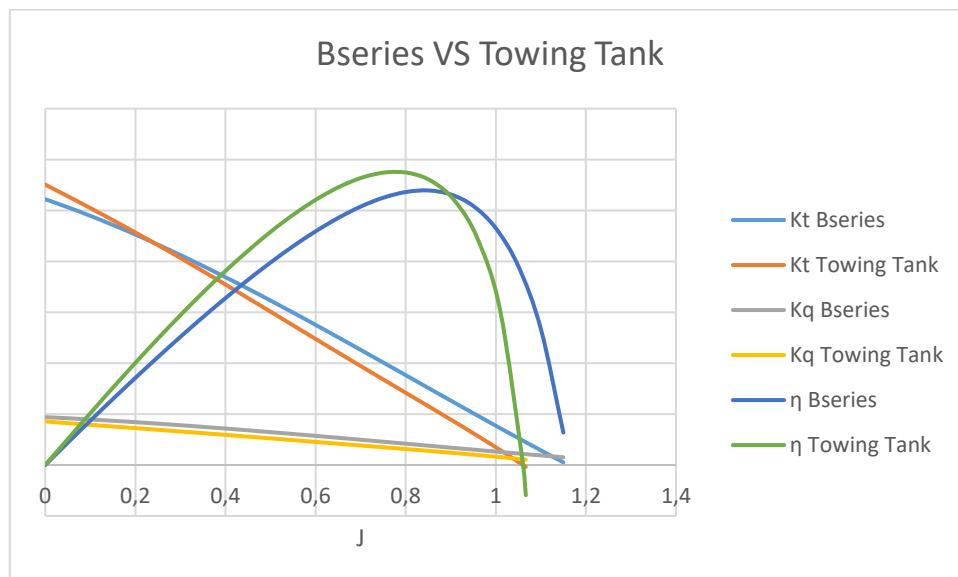


We can observe a good correlation of the curves especially for the thrust coefficient and the torque coefficient. However, regarding the efficiency  $\eta$ , a quite important gap is noticed for high advance ratio  $J$ . In our case, it will not influence the results since the advance ratio is always smaller than 1 (close to 0,93 at the convergence).

#### ➤ SHIP C

As did for SHIP B, the open curves used in CFD are also compared to the curve provided by the towing tank report. Similarly, the curves used in CFD were extracted from Bseries database using the software in FineMarine.

The results are given below.



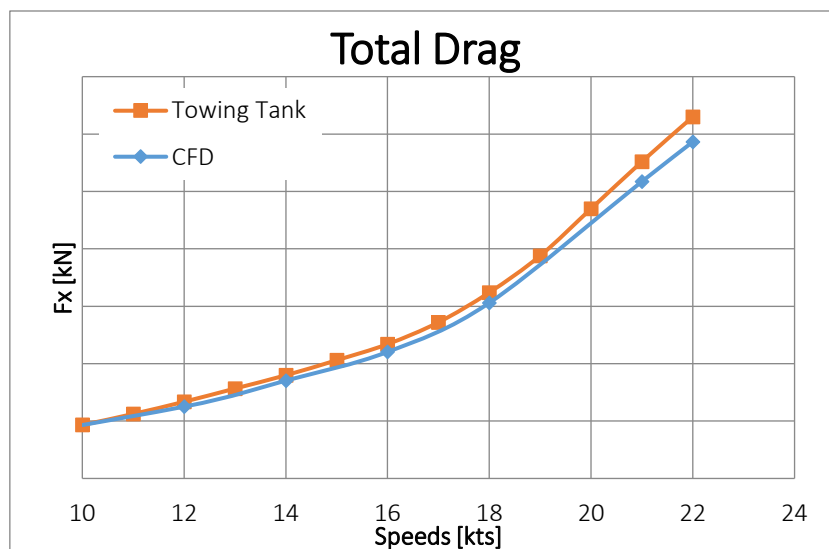
A larger error is observed on the thrust coefficient and torque coefficient between CFD and towing tank.

#### 4.3.6 Comparison results SHIP B

##### ➤ Resistance

Firstly, some simulations in resistance are done and the results are compared to the towing tank data. Only the resistance values are provided in the towing tank report. Dynamic sinkage and trim are not available.

Speeds		Fx
[kts]	Relative error [%]	
6	-1,26%	
12	-6,41%	
14	-5,18%	
16	-5,78%	
18	-5,58%	
21	-6,28%	
22	-6,92%	



The gap obtained between CFD calculation and towing tank results is around 5% for simple resistance computation.

##### ➤ Propulsion

Since close results are found in resistance, some CFD calculations in self-propulsion were done. As mentioned earlier, the actuator disk module was used with the settings defined earlier.

The results are shown.

- With the option Body Drag

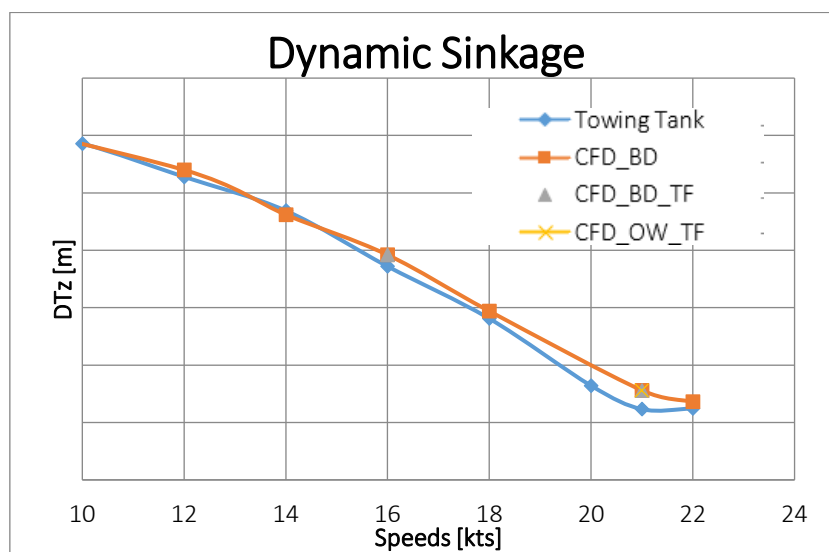
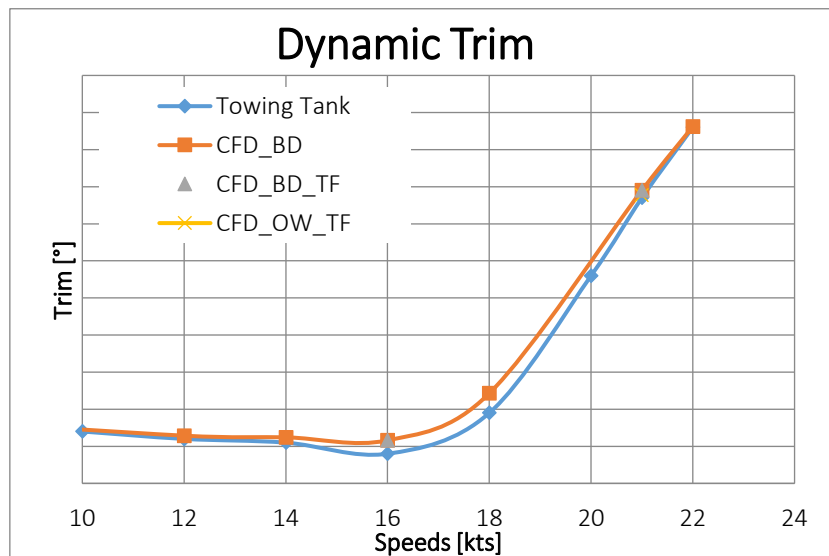
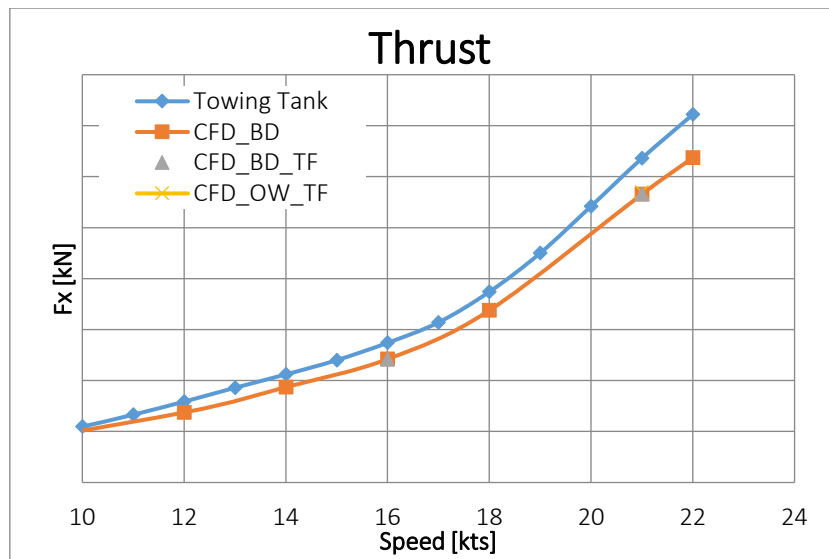
Speeds	Thrust	DTz	Ry
[kts]	Relative Error CFD/TT [%]	Absolute error CFD/TT [m]	Absolute error CFD/TT [°]
6	-15,95%	0,003	0,001
12	-13,39%	0,006	0,009
14	-11,77%	-0,003	0,014
16	-11,67%	0,010	0,036
18	-9,75%	0,007	0,053
21	-11,06%	0,016	0,020
22	-11,76%	0,006	0,002

- With the option Body Drag and the tangential forces

Speeds	Thrust	DTz	Ry
[kts]	Relative error CFD/TT [%]	Absolute error CFD/TT [m]	Absolute error CFD/TT [°]
16	-11,73%	0,010	0,04
21	-11,05%	0,016	0,02

- With the option Open-Water

Speeds	Thrust	DTz	Ry
[kts]	Relative error CFD/TT [%]	Absolute error CFD/TT [m]	Absolute error CFD/TT [°]
21	-10,16%	0,014	0,01





The gap obtained in thrust is more important than the one obtained in resistance. The error is varying around 10-15%.

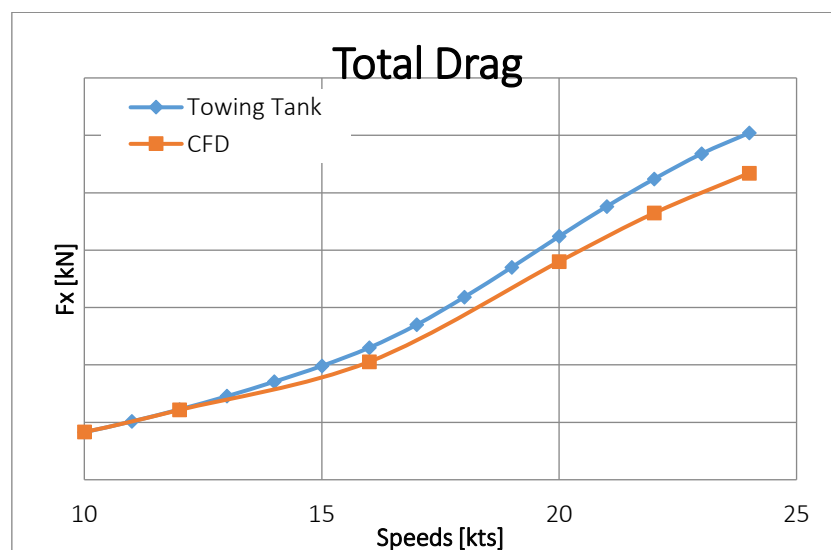
Otherwise, regarding the dynamical behaviour, the results are very similar.

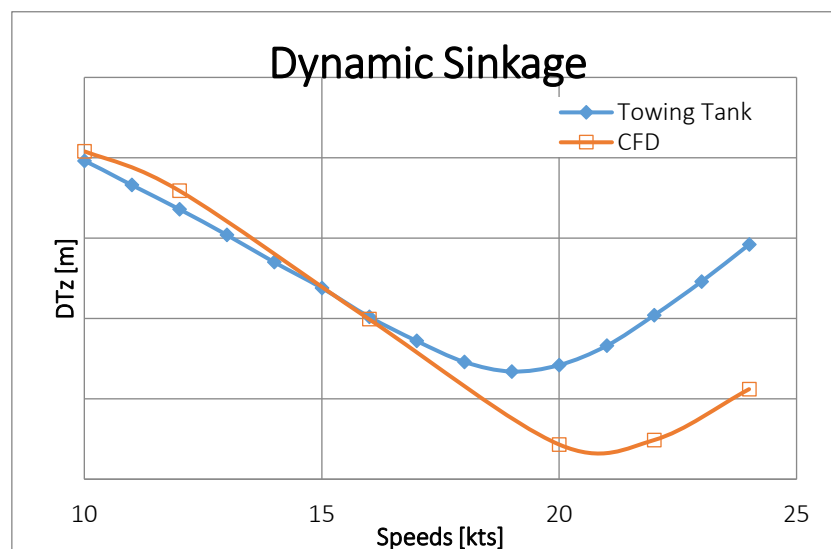
#### 4.3.7 Comparison results SHIP C

##### ➤ Resistance

Similarly, for the second patrol boat SHIP C, resistance simulations were performed to compare the results.

Speeds	Fx	DTz	Ry
[kts]	Relative error CFD/TT [%]	Absolute error CFD/TT [m]	Absolute error CFD/TT [°]
8	6,62%	0,004	-0,01
10	0,51%	0,004	-0,01
12	-0,72%	0,009	-0,01
16	-10,69%	0,001	-0,01
20	-10,36%	-0,014	0,03
22	-11,36%	-0,025	0,01
24	-11,58%	-0,027	0,02





A more important gap is observed with SHIP C than with SHIP B. Here, we can observe a relative error around 10% for high ship speed (>16%) compared to SHIP B where the errors were around 5-6%.

Furthermore, an error of dynamic sinkage of few centimetres for high ship speeds is observed. Therefore, we have decided to launch some calculations where the sinkage was imposed equal to the sinkage obtained in towing tank. The results are given in the next sections.

➤ Resistance with imposed sinkage

As mentioned in the previous section, a gap in dynamic sinkage is observed. Therefore new computations were performed in imposing the sinkage value. The results are given below.

Speeds	Fx	DTz	Ry
[kts]	Relative error CFD/TT [%]	Absolute error CFD/TT [m]	Absolute error CFD/TT [°]
12	2,09%	0	-0,008
16	11,02%	0	-0,005
22	13,31%	0	0,005

The resistance errors obtained in both configurations are given below.

Speeds	Relative error Fx CFD/TT [%]	
	Standard	Imposed Sinkage
[kts]		
12	-0,72%	-2,09%
16	-10,69%	-11,02%
20	-10,36%	-
22	-11,36%	-13,31%

We observe that the error in resistance is increasing when the sinkage is imposed. Then, this method will not be kept for the following.

After thinking, this result was quite predicable. In fact, in the classical computation, the sinkage was overestimated compared to the tank and the resistance was under-estimated. Hence, in imposing the sinkage with lower value, the wetted surface will be smaller and so the resistance will be smaller also. Therefore the gap in resistance will increase and it is what it was shown by CFD.

#### ➤ Propulsion

Despite the gap observed in the resistance CFD calculations, self-propulsion computations are also performed to compare the results to the tank results.

The results are given below.

- Option Body Drag

Speeds	T	DTz	Ry
[kts]	Relative error CFD/TT [%]	Absolute error CFD/TT [m]	Absolute error CFD/TT [°]
8	0,80%	0,003	-0,01

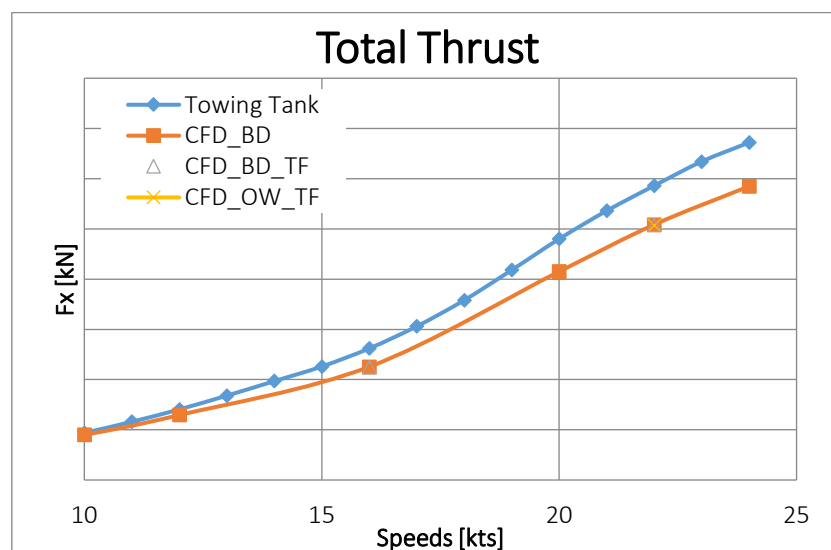
10	-4,47%	0,000	-0,02
12	-7,98%	-0,003	-0,02
16	-13,97%	-0,006	-0,05
20	-13,53%	-0,035	-0,03
22	-13,24%	-0,048	-0,04
24	-12,97%	-0,059	-0,03

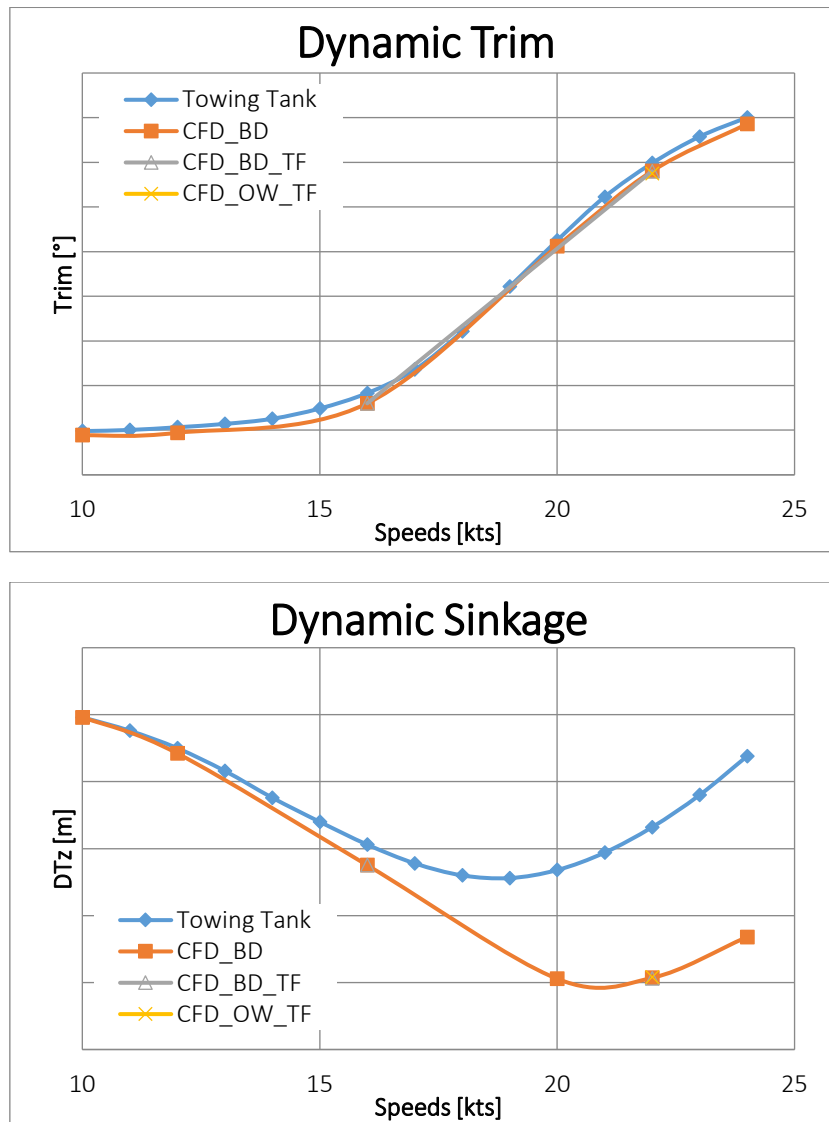
- Option Body Drag with tangential forces

Speeds	T	DTz	Ry
[kts]	Relative error CFD/TT [%]	Absolute error CFD/TT [m]	Absolute error CFD/TT [°]
16	-14,24%	-0,006	-0,05
22	-13,26%	-0,048	-0,04

- Option Open-Water

Speeds	T	DTz	Ry
[kts]	Relative error CFD/TT [%]	Absolute error CFD/TT [m]	Absolute error CFD/TT [°]
22	-13,54%	-0,047	-0,05





Similarly to what observed in the case of resistance simulation, a gap is observed for the thrust values. The order of magnitude is similar, around 10%.

The same observation is done for the dynamic sinkage. The ship is sinking much more in CFD simulation than during the tank test. I have not found any reasonable explanation about this results. In fact, the load case that is simulated is the same, it should not show as big differences.

➤ Propulsion with tangential forces

Some calculations were performed in order to study the influence of the activation of the tangential forces on the hydrodynamic results. The gaps obtained in thrust with or without the tangential forces are summed up in the table below.

Speeds [kts]	T		CPU time	
	Without TF	With TF	Without TF	With TF

<b>12</b>	-5,1%	-5,1%	6,61	8,45
<b>16</b>	2,6%	2,8%	7,34	7,29
<b>20</b>	2,8%	2,8%	7,01	7,03
<b>22</b>	3,6%	3,7%	7,14	7,13

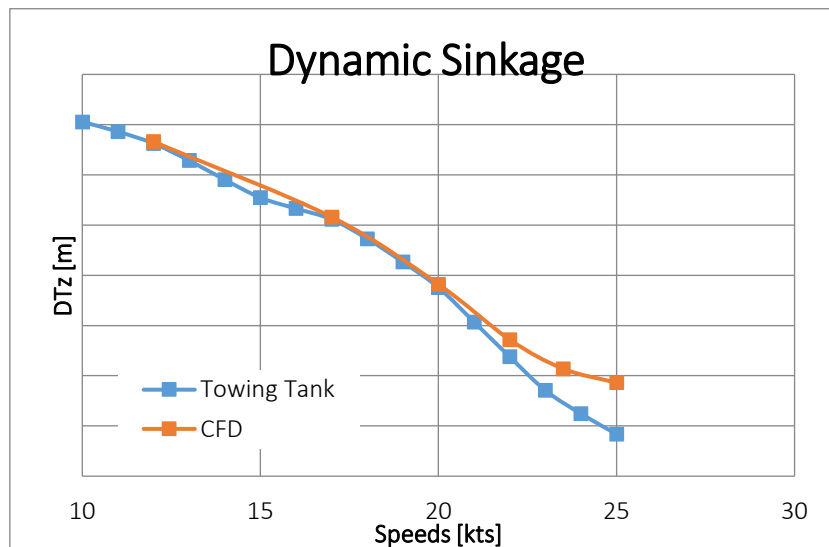
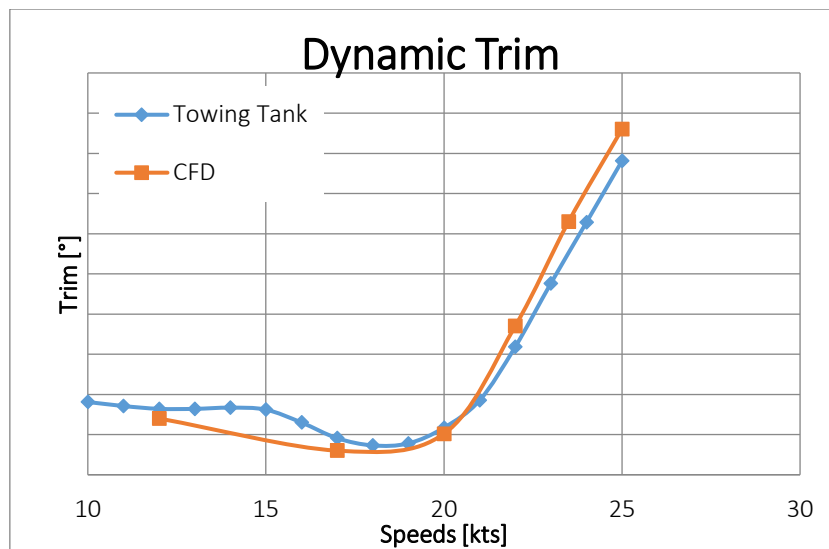
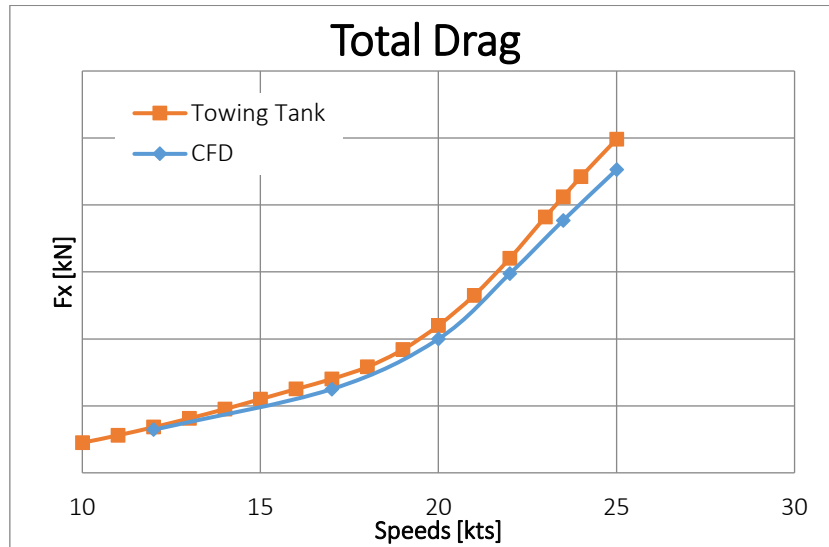
We can observe that the results are very similar whereas the tangential forces are active or not. Moreover, in term of CPU time, beyond a time much bigger for low velocity (2h more with tangential forces), the time required for the others speeds are very similar with and without the activation of the tangential forces. The main interest of the activation of the tangential forces is to get access to the torque and so to simulate the swirl due to the rotation of the propeller as it was shown in a previous section.

#### 4.3.8 Comparison results SHIP A

##### ➤ Resistance

The results obtained in resistance are given below.

Speeds	Fx	DTz	Ry
[kts]	Relative error CFD/TT [%]	Absolute error CFD/TT [m]	Absolute error CFD/TT [°]
<b>12</b>	5,6%	0,002	-0,02
<b>17</b>	10,8%	0,002	-0,03
<b>20</b>	9,1%	0,003	-0,02
<b>22</b>	7,1%	0,017	0,05
<b>23,5</b>	8,6%	-	-
<b>25</b>	9,1%	0,051	0,08

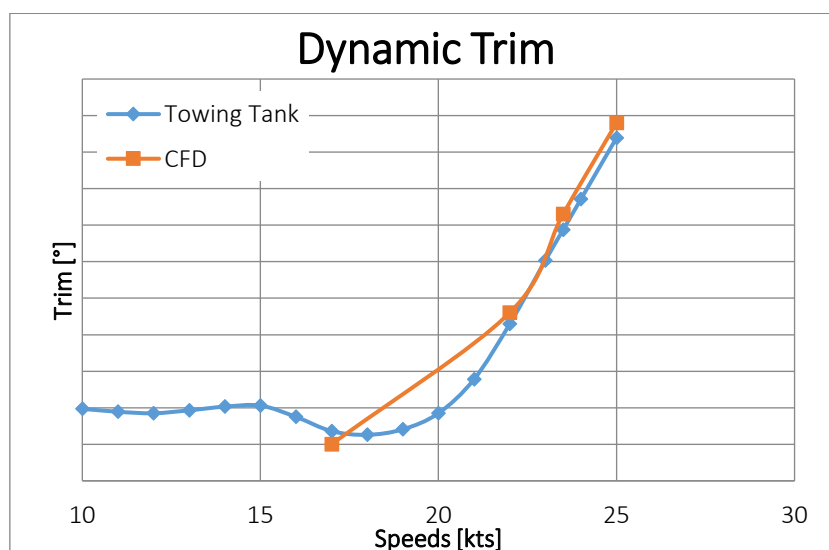
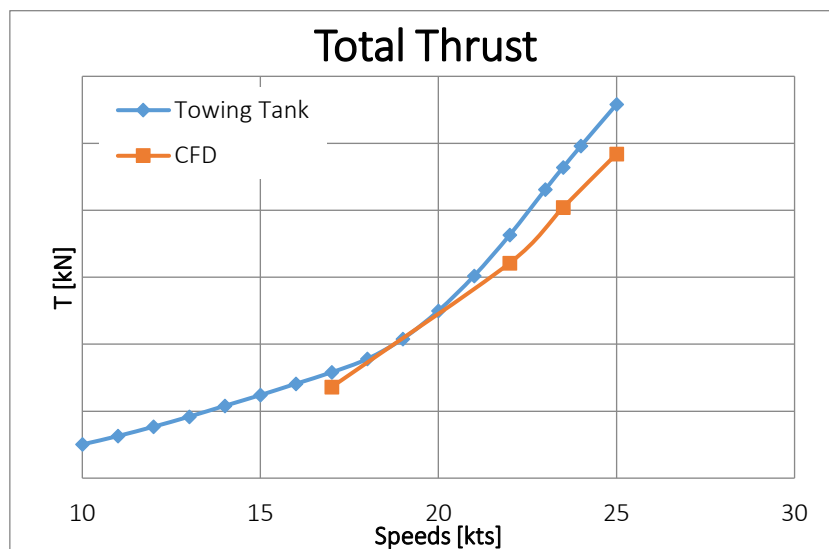


The gap in resistance is varying around 5-10% approximatively. Regarding the dynamical behaviour, the results are quite close for low speed. For large speed (larger than 22 knots) the gap is increasing.

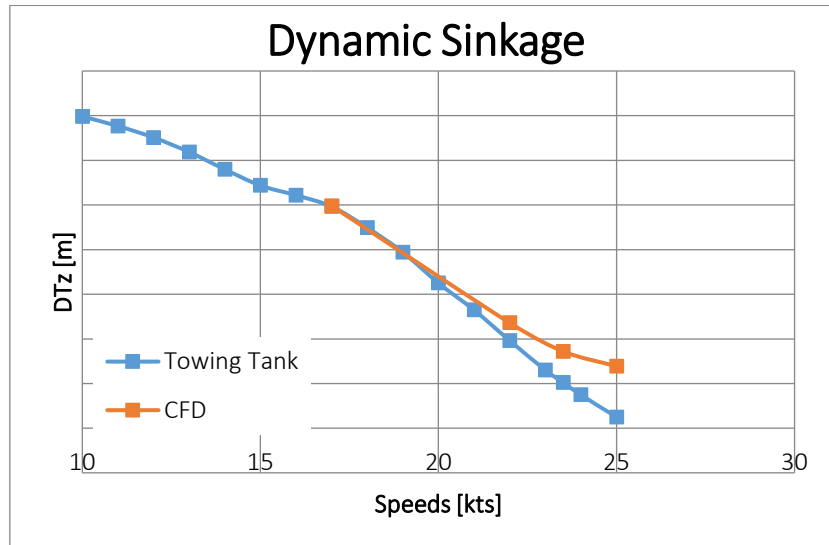
➤ Propulsion

As mention earlier, for self-propulsion simulations on SHIP A, only the option open-water was used and the results are given below.

Speeds	T	DTz	Ry
[kts]	Relative error CFD/TT [%]	Absolute error CFD/TT [m]	Absolute error CFD/TT [°]
17	12,9%	0,001	-0,04
22	11,7%	0,020	0,03
23,5	12,7%	0,035	0,04
25	13,3%	0,057	0,04







The errors observed in thrust are more important than the errors obtained in resistance (around 12% here). Regarding the dynamic behaviour, results are quite similar. For the dynamic trim the gap is very small, it is less than  $0,04^\circ$ . For the dynamic sinkage, the gap is increasing with the speed. At the largest speed 25 knots, an error of 5cm is observed, which is quite important. The ship in CFD sinks less than during towing tank test. It is explaining the error observed in thrust. In fact, if the ship in CFD would sink more, then the thrust would increase, and it would decrease the gap in thrust between CFD and towing tank.

#### 4.4 CONCLUSION

The correlation of the CFD results and the towing tank results was done in order to have an order of magnitude of the gap between them. As we know, traditionally, the towing tank results were considered as the more reliable results and all the processes were based on it. Today, CFD is becoming more and more reliable and we can think that doing CFD can be enough to conclude on power prediction and more generally on ship hydrodynamic.

The correlation was done for both resistance and self-propulsion test. Resistance is a common practice, so there were no points raised. However, regarding self-propulsion test, it is a quite new practice in the company. Even if, before some calculations were done using the actuator disk, the module in FineMarine was not very well-known and it was necessary to take some time to understand the different options and the different type of computations that can be performed. For this, I have read a lot about the possibilities with an actuator disk, about the modelling, and about the different settings. Then I have run several computations, trying the different options and comparing the results in term of physical characteristics such as Thrust, Torque, RPM but also in term of flow.

Once the module was handled, I have run the simulation with specific settings that were explained previously. The correlation shows the following results:

- In resistance, regarding the resistance, a gap of about 5-10% is observed. It is mainly increasing with the ship speed. In fact, at low speed, usually, the relative error is not so big and then the gap increases at around 17 knots. Regarding the dynamic behaviour, in most of the computations, the

values are very close to the one obtained during the tank test. So it means that in CFD, the ship motion is well represented.

- In self-propulsion, a larger gap is observed. The thrust error is around 12-13% for the three ships. Similarly to the resistance test, the dynamic behaviour is well modelled in CFD, since very close results are found in term of dynamic trim and dynamic sinkage.

In all the case, CFD results are lower than the results obtained during tank test. However, it is known that towing tank results are quite pessimistic. In fact, as it is an experimental procedure, some uncertainty considerations have to be taken into account. Usually, the errors are taken in the most pessimistic way and so it can lead to a pessimistic final results.

## 5 POWER PREDICTION METHODOLOGY

---

As mentioned earlier, the main interest of performing self-propulsion simulation is to physically represent the hull-propeller interaction. In fact, it has a strong influence on the power prediction. The hull propeller interaction is decomposed in two parts: Wake fraction and Thrust deduction factor. The definitions are given below.

- Wake fraction coefficient  $w$  [8]

A boundary layer around the hull is created when the ship is advancing. In this layer, the velocity of water on the surface of the hull is equal to the velocity of the ship. But this velocity of water reduces with its distance to the hull. Outside of the boundary layer, the velocity of the water is equal to zero. Moreover, this boundary layer is increasing in terms of thickness along the hull (thicker at the aft part than at the fore part). Therefore, the propeller will be working on the wake of the ship. It means that at the propeller plane, the water will have an effective wake velocity. We call Advance velocity  $V_A$ , the average velocity that the propeller is encounter in reality which is smaller than the ship velocity  $V$ . The wake factor is then equal to:

$$w = \frac{V - V_A}{V}$$

- Thrust deduction factor [8]

Due to the rotation of the propeller, the water in front of the propeller will be sucked back toward the propeller and it will induce an extra resistance to the hull called “augment of resistance”. Therefore the total required thrust force of the propeller needs to overcome the ship resistance  $R_T$  and this loss of thrust. The thrust deduction formula is then given by:

$$t = \frac{T - R_T}{T}$$

Below, the power prediction methodology is shown from resistance test results. Then, it will adapted to our self-propulsion calculation using the thrust values directly.

### 5.1 CLASSICAL METHODOLOGY BASED ON RESISTANCE SIMULATION

The powering law is defined below. It represents the ratio between the effective power (real power) and the power delivered by the engine.

$$\frac{P_E}{P_I} = \frac{P_E P_T P_D}{P_T P_D P_S}$$

Where:

- $P_E = RV$  : Effective Power
- $P_T = TV_A$  : Delivered Power by the propeller
- $P_D = 2\pi Q_s n$  : Transmitted power to the propeller
- $P_S = 2\pi Mn$  : Power output of the engine

The efficiency is equal to the previously mentioned ration. It is the relation between the effective power (EHP) which is the required power to move the ship at certain speed and the brake power horse power of the engine (BHP). It is divided in few terms defined below [8]:

- Hull efficiency  $\eta_H$ : It is equal to the ratio between the effective power and the thrust power

$$\eta_h = \frac{1 - t}{1 - w}$$

Where:

- $t$ : Thrust deduction factor
- $w$ : Wake fraction coefficient
- Open water propeller efficiency  $\eta_0$ : It is related to the situation when the propeller works in an open-water environment (homogeneous wake field). Usually it is given by the open-water curves from experiments. It is given by the following theoretical formula:

$$\eta_0 = \frac{K_T J}{K_Q 2\pi}$$

Where:

- $J$ : Coefficient of advance ( $J = \frac{U}{nD_p}$ )
- $K_T$ : Thrust coefficient
- $K_Q$ : Torque coefficient
- Relative rotative efficiency  $\eta_R$ : The water that is flowing through the propeller is no as uniform as during open-water test. Due to the presence of the hull, it has a rotational flow. Therefore the propeller's efficiency will be affected by this factor  $\eta_R$ .
- Mechanical losses  $\eta_S$ : The shaft efficiency depends mainly on the lubrication of the bearings, the alignment and the choice of the gearbox.

The overall efficiency is then given by the following formula:

$$\eta_t (OPC) = \eta_H (\eta_0 \eta_R) \eta_S$$

The complete powering law is considered when wanted to estimate the power based on resistance CFD calculation. The resistance is considered as an output of the CFD calculation.

In general, the aerodynamic drag imposed by the superstructure is also taken into account. It is added to the ship drag computed by CFD. It is computed using the following formula:

$$R_{aéro} = \frac{1}{2} \rho S V^2 C_x$$

## 5.2 ADAPTATION WITH SELF-PROPULSION CFD

When doing self-propulsion CFD calculation, the propulsion system is modelled by an actuator disk. The output is not anymore the resistance by the thrust of the propeller required to reach the target speed. It means that this method allows to get access to the delivered power without requiring the effective power. The interaction between the hull and propeller is directly taken into account via the integration of the propeller (actuator disk).

The calculation of the delivered power has to be done as function of the advance velocity (flow velocity near the propeller) and not as function of the ship speed. This velocity can be extracted through the advance coefficient, output data of the CFD computation. So we have:

$$P_T = TV_A = TJnD$$

Where:

- T : Thrust (kN)
- J : Advanced coefficient
- N : Propeller rotation speed (rps)
- D : Propeller diameter

T, n et J are output data of the CFD calculation in self-propulsion

Once this power is computed, the other powers can be computed based on their respective efficiencies presented in the previous section.

$$P_D = P_T \eta_0 \eta_R$$

$$P_S = P_D \eta_S$$

## 5.3 RESULTS

For each ship, the required power is computed based on three different methods:

- Towing Tank results
- Power estimation from resistance CFD
- Power estimation from self-propulsion CFD

A margin of 5% is applied for CFD that corresponds to the gap observed during CFD resistance calculations.

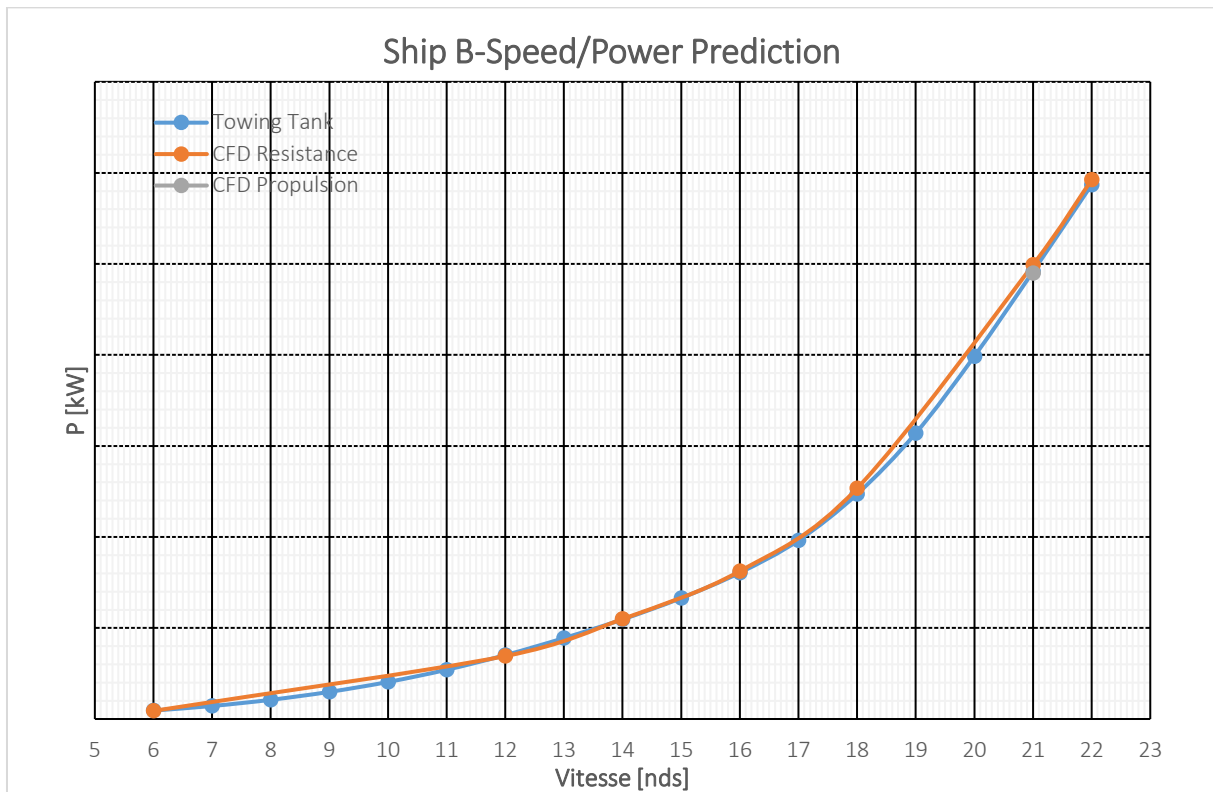
### 5.3.1 Results SHIP B

The efficiencies that are considered are shown below.

Efficiencies	
Wake : 1-wt	98%
Thrust factor : 1-t	90%
$\eta_0$	69%
$\eta_R$	97,5%
Perte Mécanique	96%
OPC total	59.3%

The power  $P_S$  obtained are shown in the table below.

Speed	Towing Tank	CFD Resistance		CFD Propulsion		
		Power	Error/TT	Power	Error/TT	Error/Resistance CFD
[nds]	[kW]	[kW]	[%]	[kW]	[%]	[%]
6	92,70	89,46	3,5%	-	-	-
12	702,00	691,17	1,5%	-	-	-
14	1094,00	1099,50	-0,5%	-	-	-
16	1607,00	1624,97	-1,1%	-	-	-
18	2471,00	2534,33	-2,6%	-	-	-
21	4915,00	4989,49	-1,5%	4896,70	0,37%	1,86%
22	5870,00	5923,45	-0,91%	-	-	-



We can observe a good correlation of the results between the tank data and the power prediction made using CFD results. The results obtained in self propulsion are very close to the one obtained using the classical method.

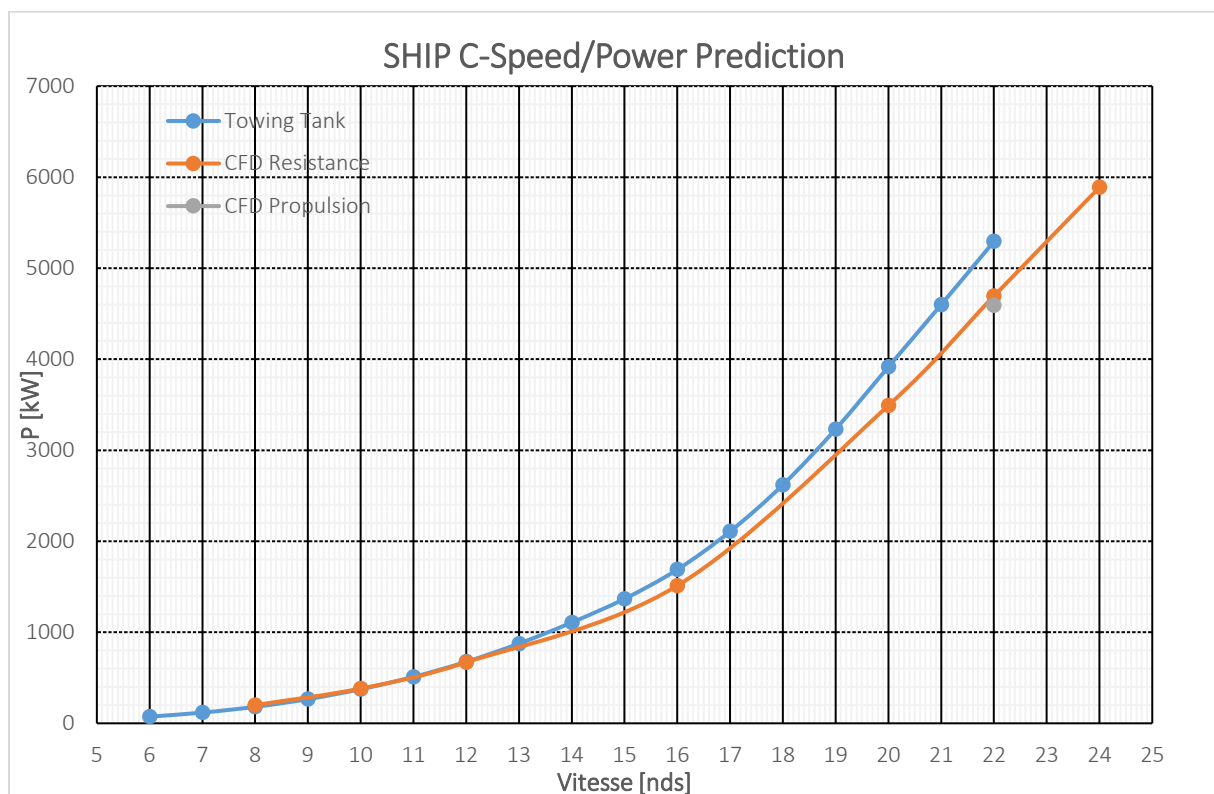
### 5.3.2 Results SHIP C

The efficiencies are shown below.

Efficacités	
Wake : 1-wt	98%
Thrust factor : 1-t	90%
$\eta_0$	69%
$\eta_R$	97,5%
Perte Mécanique	96%
OPC total	59.3%

The power  $P_S$  obtained are shown in the table below.

Speed	Towing Tank	CFD Resistance		CFD Propulsion		
		Power	Error/Towing Tank	Power	Error/Towing Tank	Error/Resistance CFD
[nds]	[kW]	[kW]	[%]	[kW]	[%]	[%]
8	181	200,05	-10,53%			
10	375	382,82	-2,09%			
12	676	670,65	0,79%			
16	1689	1512,34	10,46%			
20	3916	3492,15	10,82%			
22	5294	4694,20	11,33%	4591,66	13,27%	2,18%
24	6643	5889,37	11,34%			



The results obtained from self-propulsion CFD are very close to the one obtained using the classical resistance CFD. The error observed between the power predicted by CFD and the one computed by the towing tank is larger than with SHIP B. It is due to the fact that from the beginning, 10% errors were found during simple resistance CFD.



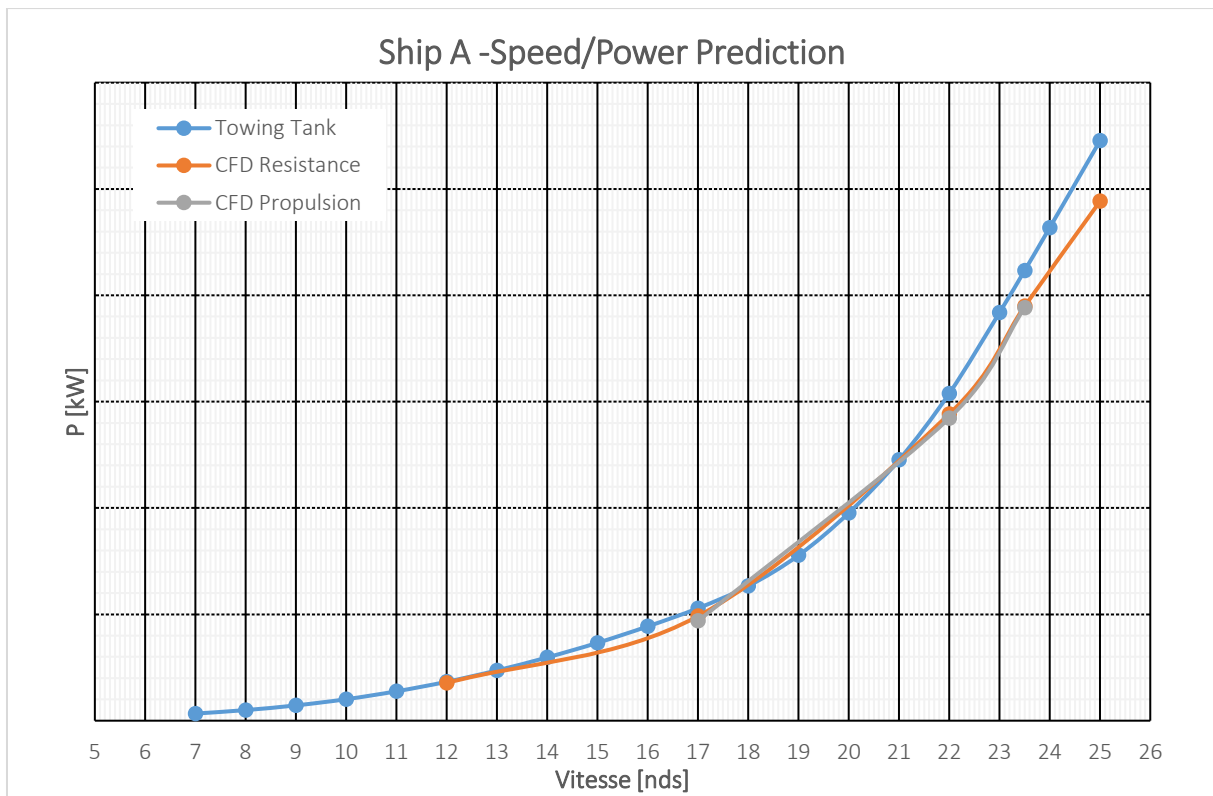
### 5.3.3 Results SHIP A

The efficiencies are shown below.

Efficacités	
Sillage : 1-wt	98%
Succion : 1-t	90%
Rendement Hélice	69.5%
Efficacité Rotation	97,5%
Perte Mécanique	96%
Pertes SS	100%
OPC total	59.7%

The power  $P_5$  obtained are shown in the table below.

Speed	Towing Tank	CFD Resistance		CFD Propulsion		
	Power	Power	Error/Towing Tank	Power	Error/Towing Tank	Error/Resistance CFD
[nds]	[kW]	[kW]	[%]	[kW]	[%]	[%]
7	133,3					
12	731,25	708,88	3,1%			
17	2114,58	1964,79	7,1%	1875,25	11,36%	4,13%
22	6153,13	5767,57	6,3%	5693,54	7,51%	1,33%
23,5	8464,58	7792,96	7,9%	7768,34	8,27%	0,36%
25	10907,29	9768,00	10,4%			



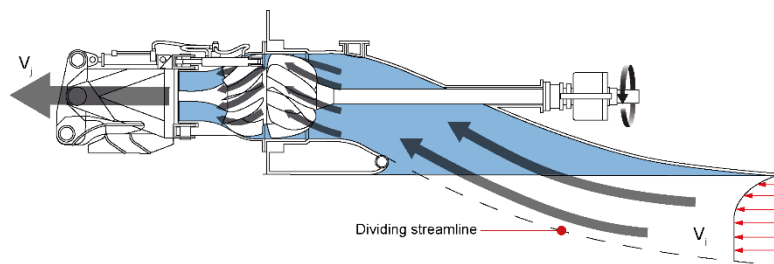
The correlation is quite good.

## 6 AUXILIARY COMPUTATIONS

### 6.1 WATER-JET SIMULATION

In this section, some simulations with water-jet will be performed within the framework of a currently designed ship. The water-jet is a very specific system and there is not a lot of documentation about the simulation of water-jet in CFD.

A water-jet is a marine system that produces a jet of water for propulsion [9] mainly used for fast ship. The design is shown below.

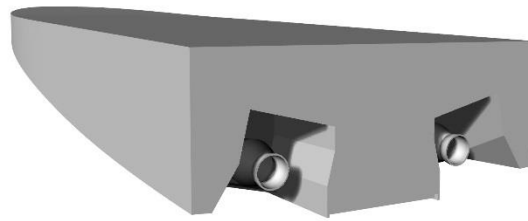


*Water-jet design*

As we can see, it incorporates an intake, where the flow is accelerated and propelled to the stern thanks to an impeller/stator system which induce a thrust force. The system requires a specific layout. For CFD calculation, to make things simpler, only the duct was designed. Hence the nozzle, the impeller/stator and the shaft were forgotten.

An actuator disk is used and placed at the location of the impeller/stator system. The data available for the geometry of the system were not very precise, but it does not matter, since here the interest is to visualize the flow from the intake to the stern of the ship. The 3D model of the water-jet is shown on the images below.



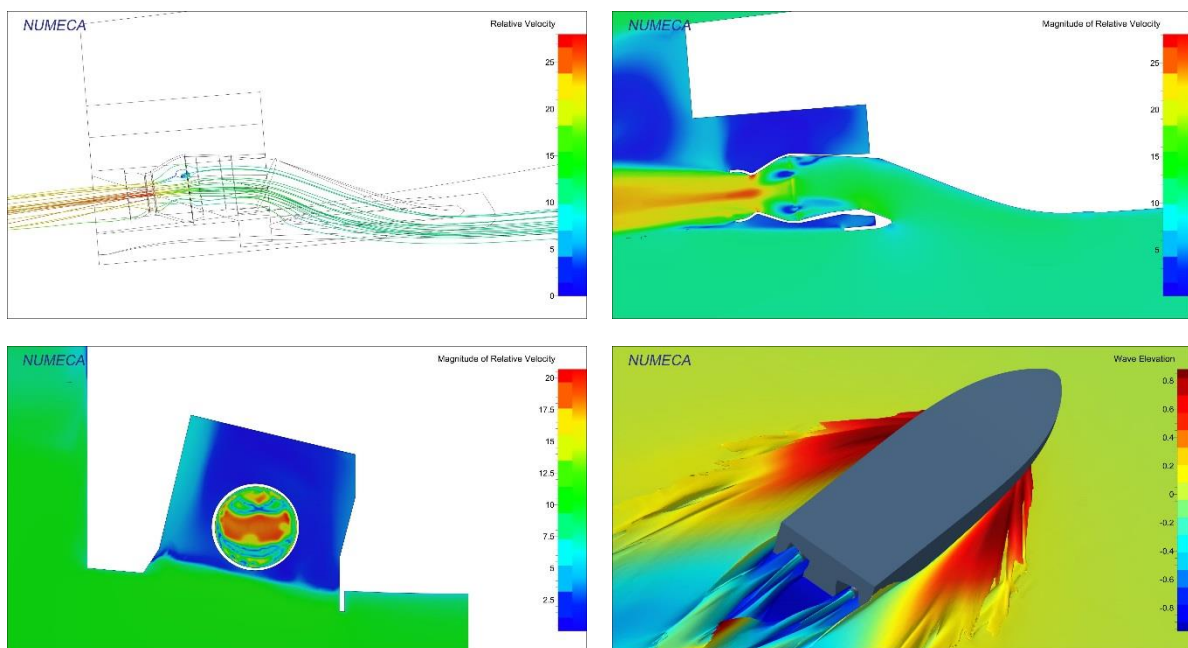


*Water-jet 3D model: Bottom view (Top left corner), Stern view (Top right corner), Perspective view (Bottom)*

In the module Actuator Disk on FineMarine, the standard configuration was used: Body Self-Update/Body Drag without tangential force. In fact, as no information are provided about the water-jet, it is the only configuration that is applicable. The tangential forces cannot be active since no data about the torque are available and so no initial values can be set. The force distribution chosen is the uniform one. Indeed, since the flow is inside a duct, it will be concentrated and so spread uniformly over the surface of the disk.

The simulation was done for one ship speed, 20 knots, and for two configurations (with and without interceptor). The most interesting point is the flow visualization near the intake.

Below, some images of the flow are given but only for one configuration (without interceptor).

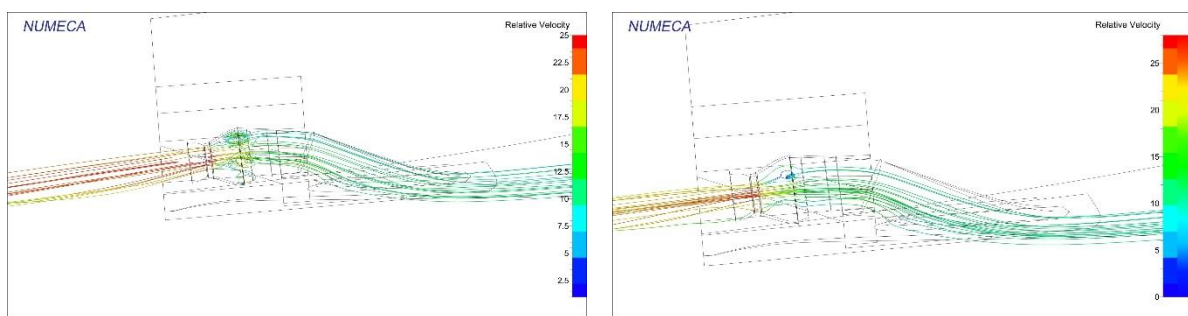


On the first image, we can observe the flow entering the duct by visualizing the streamlines. We can observe that there are some vortices that are created where the duct becomes wider (location of the impeller). It

means that the circulation of the flow is not so good. It might be due to the fact that the real shape of the impeller/stator cannot be represented. Indeed, in the reality, the impeller/stator takes the shape of the duct on a given thickness. For the numerical simulation, only a cylinder can be represented, so there is two solution:

- The maximal radius is kept and so the thickness is taken as very small
- The thickness is kept, and so the radius is adapted so that the cylinder is inside the duct without interception

The second solution was considered first. However it was given larger vortices since the disk was not taking the full section of the duct. Moreover, because of these vortices, the thrust/resistance could not get stabilized, it was oscillating around a fixed value. Hence, we decided to use a very thin disk that is taking the full section. This solution reduces the vortices in the duct, and it allows to have a good convergence of the results (thrust, resistance and dynamic behavior).



*Streamlines in the duct with the two configurations: Thick disk (Left), Thin disk (Right)*

On the second and fourth images, we can observe the acceleration of the flow. It is shown that the flow is mainly accelerate at the horizontal central plane of the disk. It means that the flow is mainly concentrated at the middle of the duct. So at the intake, the flow is not coming homogenously, there are some loses at the front and aft connection. Maybe the intake is too sharp, and so the flow cannot follow the shape of the intake.

On the fourth image, the wave elevation is represented. We can see that the two jets are outside the water and we can clearly observe that the water is well reject out of the jet.

## 6.2 RESISTANCE ON REGULAR WAVE WITH ACTUATOR DISK

Resistance on regular wave calculation was done for two different ships. Two different types of calculations were performed:

- Fixed point: In this computation, the ship is fixed and the waves are generated through an internal wave generator. In this case, the module “internal wave generator” have to be used. According to Numeca, “the internal wave generator creates waves in the domain based on a momentum source term applied to the Navier-Stokes equations. More natural than imposing a wave generator on a boundary conditions, it ensures a clean wave signal at all times.” [1].
- With advance speed: In this computation, the ship is moving (by imposing surge motion or with an actuator disk). A wave generator is then imposed on a boundary condition (Xmax if head seas).

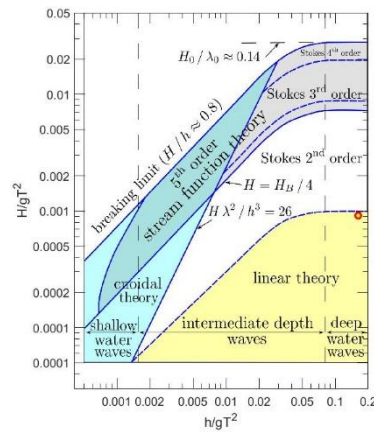
Only the results obtained with SHIP A, on head seas, regular wave, are presented in this report (second configuration).

The regular wave model, also called Airy wave model, is obtained by considering the linear theory from Stokes equations. The main assumptions are that the steepness is very small compared to 1 (small slopes) and that the waves are dispersive (follow a dispersion relation). It is based on potential flow theory to describe the movement of gravity waves at the free surface [1].

A CFD calculation on regular wave was done on the patrol boat SHIP A in order to have an idea on the added resistance due to the wave. The wave characteristics are given below:

- Period: 8.3s
- Wave height: 0.6m

Based on the above characteristics, a linear model of regular wave can be applied. It can be checked based on Le Méhauté plot which gives the limits of the different Stokes order.



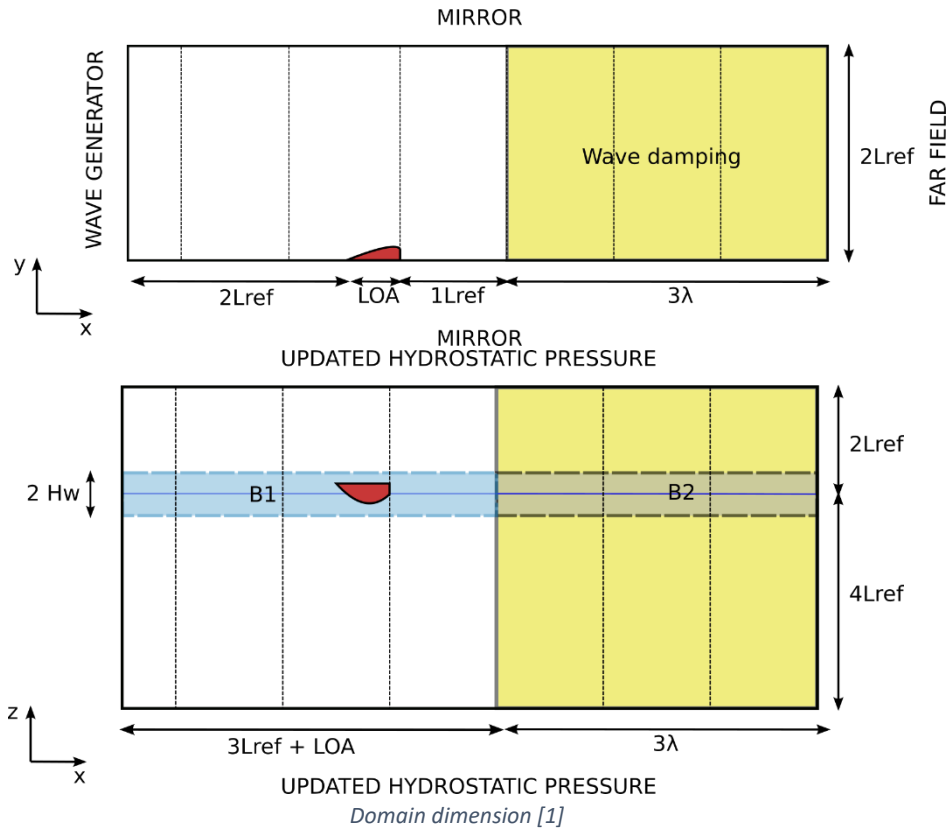
The steepness coefficient  $\epsilon$  is given by the following equation:

$$\epsilon = kA = 0.018 \ll 1$$

The dispersion coefficient  $\mu$  is given by:

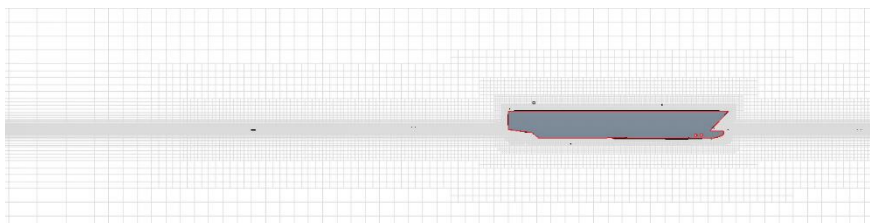
$$\mu = kd = 6.4$$

The initial domain is slightly different than for a classic resistance calculation. It has to be adapted due to the wave generation. The domain sizes prescribe by Numeca are given below.



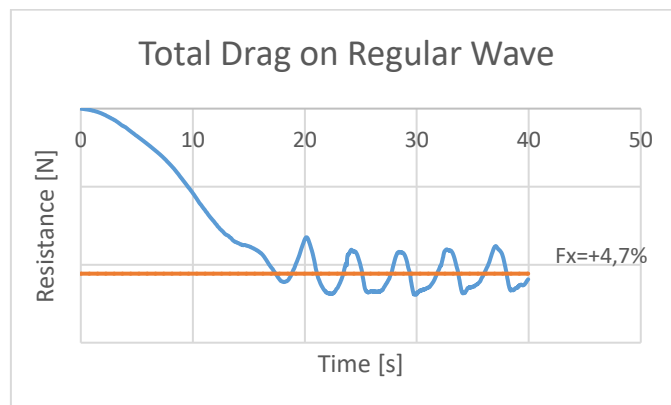
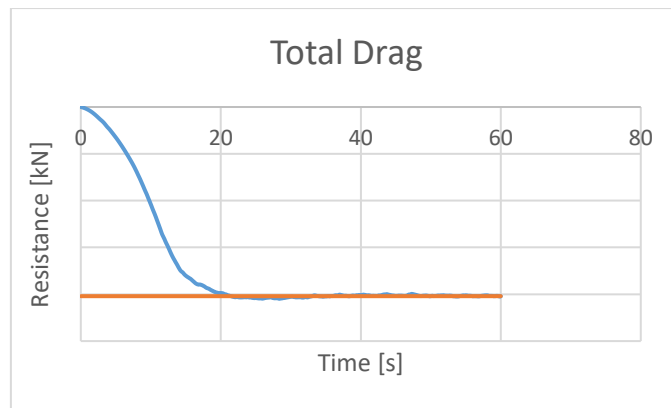
- The domain is much bigger especially in X and Z.
- A zone around the ship has to be refined nearby the free surface (as usual, but finer)
- A large zone behind the ship has to be defined in order to damp the generated wave which corresponds to three times the wavelength. It is done to avoid any reflection of the wave on the  $X_{min}$  boundary. It is made in coarsen the mesh in X direction (no refinement in X). It is well observable on the lateral view of the mesh below. The module “Wave Damping” of FineMarine is used in parallel. It adds a sponge layer as a sponge layer that damp the free surface waves to avoid as well any undesired reflection on the boundaries. It acts as porous media that damp the momentum in Z direction.
- Both lateral boundaries ( $Y_{min}/Y_{max}$ ) are set as mirror boundary in order to avoid any reflection of the wave which can interfere with the generated wave and give unwanted results.
- The wave generator is located in the  $X_{max}$  face. The boundary condition has to be set as “Wave Generator”.

A lateral view of the mesh is shown below.



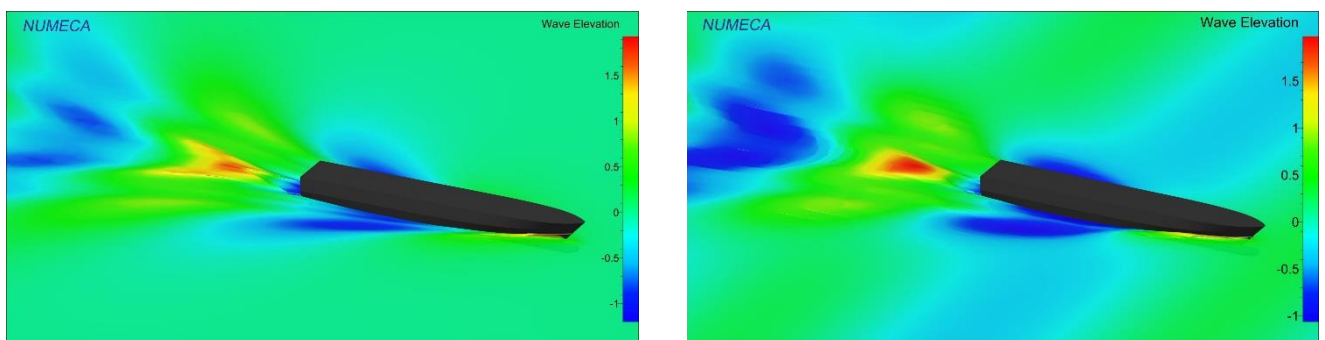
*Side view of the mesh – refinement around the free surface*

The results obtained are shown below. The calculation was launched for a ship speed equals to 23,5 knots. As the induced resistance is requested, only the total drag is shown.



The simulation was done in two parts. The first three iterations correspond to a simulation where the ship speed was imposed. Then the speed was released and the rotation speed of the disk was imposed. More iterations would be required normally, however, it takes a long time to run, and we did not have enough time to simulate more periods. Indeed, the simulation was launched for almost 90h just to simulate 5 wave periods.

Regarding the results, it can be seen that the regular wave is inducing an increase of mean resistance of about 4,7%.



SHIP A CFD: Calm water (Left) and regular wave (Right)

On the image above, we can clearly distinct the simulation in calm water (left) and in regular wave (right). The wavelength is quite long (107 m) it is why only two wavelengths are visible in the image. The wake of the ship is quite similar between the two configurations.



## 6.3 BOLLARD PULL CALCULATION

Bollard pull is a conventional measure of the pulling (or towing) power of a watercraft. It is defined as the force exerted by a vessel under full power [10].

In this case, bollard pull configuration was used in order to estimate if some ventilation phenomena would occur when the ship tries to get out of a beach by going backward. It was tested on an Amphibious Landing Craft. So it is regularly accosted on a beach.

Ventilation occurs when a negative pressure at the propeller tip will be sufficient to create suction of the free surface up to the blade. And so surface air are pulled into boat propeller blade. It can induced a loose of thrust of the propeller.

The modelling used is described below.

- The ship is going backward
- Actuator disk defined imposing the rotation rate of the propeller
- A mooring line located at the bow of the ship modelling the attachment of the ship with the beach. The stiffness of the mooring line is defined based on the required thrust and the formula is given below.

$$k = \frac{2 * Thrust_{AD}}{0.1} [N.m]$$

- No streaking correction imposed → Otherwise it will hide the ventilation phenomena

As we can see some simplifications of the real situation are made. Indeed, the beach itself is not represented and the calculation is done in deep water condition. The very shallow water condition and the large contact area might have a big influence on the results and may induce other phenomena that are neglected in our model.

In this case, the ship was tested for two different rotation rate (400 and 600 rpm) with two different configurations:

- First configuration: Without tangential force → The propeller rotation is not represented (simulation for 400 and 600 rpm)
- Second configuration: With tangential force → The propeller rotation is represented (only for 600 rpm).

Then, a couple of data are post-processed such that:

- the flow
- the thrust evolution
- the tension in the mooring lines

The results are shown in the following sections only for the second configuration (tangential force/rotation of the propeller).

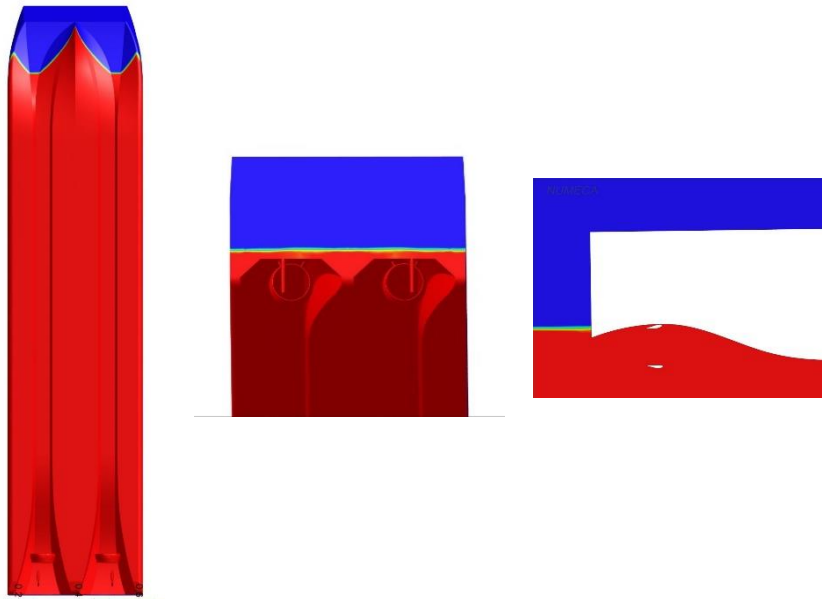
### 6.3.1 Simulation for 600 RPM with axial and tangential forces

A simulation with the modelling of the propeller rotation was realized. In fact, it allows to represent more realistically the flow in the propeller area. The input data is here the rotation speed (i.e. 600 rpm).

The following configuration of the actuator disk was used:

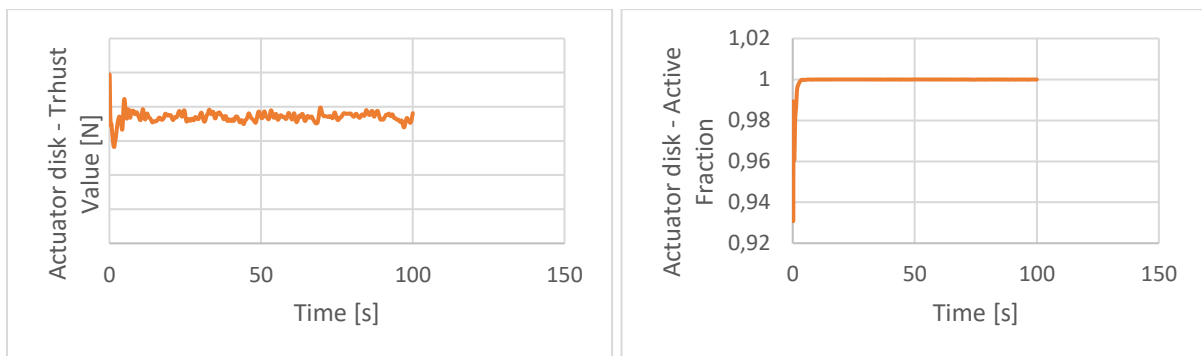
- No body force update: The required thrust (knowing the rotation speed) is directly applied to the disk.
- The tangential force are active
- The direction of the disk is reversed to make the ship going backward.

Below, the pictures show the mass fraction computed on the hull.



*Mass fraction: From below (LEFT), from behind (MIDDLE), in the propeller plane (RIGHT)*

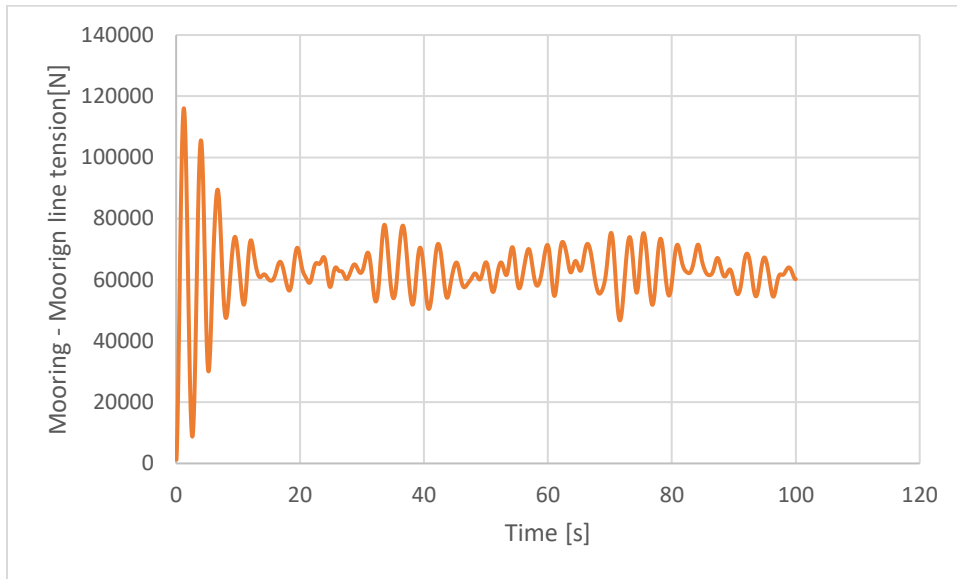
It is clear to say that there is no risk of ventilation in this configuration.



*Thrust (left) and active fraction (right) convergence*

Mean Effort	
Thrust	37 kN
Active Fraction	1

The thrust is stabilizing around a mean value of 37kN. And the active fraction is equal to 1.



*Convergence of the mooring line tension*

Above, the figure represents the tension in the mooring line. A strong oscillatory comportment is visible due to the thrust variation.

## 6.4 MANOEUVRABILITY (TURNING CIRCLE)

A manoeuvrability question was raised regarding the currently designed patrol boat SHIP A. Hence, a CFD simulation of a turning circle was performed in order to have a look on the gyration radius. The main particularity of this simulation is that the rudders have to rotate during the simulation and therefore the rudders have to be mesh in a different domain than the hull. The overset grid option is then used to interpolate both mesh together. The overset allows the interpolation of the fluids between two domains that are overlapping [1].

Moreover, since the ship will rotate, the full hull has to be mesh. In simple resistance test, since the simulation is symmetrical along x axis, only half body was meshed. Here the full model (full appended) is meshed and so it is much more costly. During self-propulsion calculation, the number of cells was close to  $6,9 \cdot 10^6$ . Here, it is close to  $12,9 \cdot 10^6$ .

An actuator disk is used to simulate the ship propulsion. The settings are similar to the one used during self-propulsion calculations for SHIP A.

The simulation is divided in three parts:

- First, the velocity is imposed and the ship is advancing until reaching a steady state. It is called the flow initialization. In this stage, the ship is free to trim and sink. The others degrees of freedom are blocked.

- Secondly, restarting from the first stage, the rpm is imposed to both actuator disks. This phase is called the rudder execution stage. A rotation is imposed to the rudders to reach its final position ( $35^\circ$ ). As the ship will start to turn, all the degrees of freedom are free.
- Lastly, once the rudders reached its final position, the rudder position is fixed, and the rpm is still imposed. This stage is called the constant rudders angle phase. It has to be run until the ship have completed the full turning circle. In this stage, all the degrees of freedom are still free.

Finally, we had not enough time to launch the simulation.

## 7 DISCUSSION/CONCLUSION

---

During this 6 month period in Mauric, I have been very well integrated in the company, and I had the opportunity to collaborate in the current projects.

The main topic of my thesis was to develop a methodology to perform CFD calculation in self-propulsion using Actuator Disk. Firstly, I took time to learn about the Actuator disk, to understand how it works and to figure out the different settings in FineMarine. Then, several computations were performed to correlate the result with towing tank results that were performed previously.

Once the module was handled, I had the opportunity to perform similar calculations on current projects. Self-propulsion calculations were performed on the currently designed patrol boat and the results were correlated to the towing test results that were done during the same period. Furthermore, auxiliary CFD calculations were performed using the actuator disk, such that resistance test on regular wave, bollard pull test, and manoeuvrability simulation.

From a personal point of view, this internship was very interesting. I was trained on FineMarine. I am now able to use the three main software of FineMarine which are Hexpress (grid generator), ISIS solver and CFview. These software are complementary and allow to solve a hydrodynamic problem. After having handled the actuator disk module, it was really interesting to apply it to others subjects.

From a professional point of view, it allows me to have a general vision of a ship design project, from the tender stage to the delivery to the shipyard. I was more focused on the hydrodynamic parts of a project. I had the opportunity to write some reports summarizing the different CFD computations done throughout the design process (from the tender hull form to the final one used for the towing test). It was really interesting to have a look on it, to understand how the hull is shaped and how the decision is making.

Regarding the company, I think now self-propulsion CFD calculations can be performed. I wrote some documents explaining the different configurations and settings of the module Actuator Disk in FineMarine.

## 8 REFERENCES

---

- [1] Numeca, "FineMarine User Guide," [Online]. Available: <https://portal.numeca.be/docs/Default.htm>.
- [2] M. Javadi, "Experimental Investigation of the Effect of Bow Profiles on Resistance of an Underwater Vehicle in Free Surface Motion".
- [3] Woods Hole Oceanographic Institution for the Bureau of Ships, Marine fouling and its prevention.
- [4] V. I. Krasilnikov, "Self-Propulsion RANS Computations with a Single-Screw Container".
- [5] D. Villa, "Ship Self Propulsion with different CFD methods: from actuator disk to viscous/inviscid unsteady coupled solvers".
- [6] H. Jasak, "CFD validation and grid sensitivity studies of full scale ship self".
- [7] B. Šeb, "NUMERICAL CHARACTERISATION OF A SHIP".
- [8] J. Ghose, Basic Ship Propulsion.
- [9] "Water-jet," [Online]. Available: <https://en.wikipedia.org/wiki/Pump-jet>.
- [10] "Bollard Pull," [Online]. Available: [https://en.wikipedia.org/wiki/Bollard\\_pull](https://en.wikipedia.org/wiki/Bollard_pull).